Chapter 1 Introduction

1-1Background

Recently developed artificial media, called the left-hand-materials, with simultaneously negative values of effective permeability m_{eff} and permittivity e_{eff} have received much interest [1-4]. These left-hand-materials exhibit unusual properties such as negative index of refraction, antiparallel wave vector and Poynting vector [5]. Smith et al [3] found that in a frequency region both m_{eff} and e_{eff} were negative and refraction index was unambiguously negative. Shelby *et al* [4] demonstrated that an electromagnetic (EM) wave undergoes negative refraction in a prism made by the left-hand-materials. In particular, it has been suggested that negative refraction leads to a superlensing effect that can overcome the diffraction limit inherent in conventional lenses [1]. These phenomena have been investigated and at the moment only appear possible in the microwave regime. To explore the negative refraction in the optical regime, one may turn to a photonic crystal (PC) as interesting alternative. Experimental [6] and theoretical works [7] indicate that the negative refraction phenomenon in PC are possible in regimes of negative group velocity and negative effective index above the first band near the band edge.

In 2003, Costas Soukoulis and colleagues at Iowa State University in the US and the FORTH laboratory in Greek performed computer simulations on a left-handed photonic crystal to show that causality remains intact in such materials [8]. The researchers solved Maxwell's equations to study how an electromagnetic wave evolves in time as it hits the surface of a negative-index material. They saw that the incoming beam was refracted in the negative direction - as expected - but they also noticed that this refraction did not occur straight away. Instead, the whole wave front was temporarily trapped in the surface region. Soukoulis and colleagues argue that the delays caused by this trapping explain how the outer rays in the beam *appear* to travel faster than the velocity of light.

"These calculations are an important confirmation that the speed of light is not violated by

negative refraction," John Pendry, a theorist at Imperial College in London who did much of the early work on negative-index materials, told us. "It is time to move on and start making use of these amazing new materials." Further experiments and simulations confirming the existence of negative-index materials have been performed by Claudio Parazzoli and co-workers at the Boeing Phantom Works in Seattle [9], and by Andrew Houck and colleagues at Harvard University and the Massachusetts Institute of Technology.

1-2 Motivation

There are several applications for negative refractive index material. We can't anticipate specific examples, yet. We believe that when one creates a new material that scatters electromagnetic radiation in a unique manner, some useful purpose will be found. We can envision, for example, uses in the cellular communications industry, where novel filters, antennas, and other electromagnetic devices are of great importance. Even slight improvements to these devices can make a significant financial impact.

In this paper, we measure the EM wave propagation through the photonic crystal prism to find the refraction phenomenon in microwave regime; the other, we simulate the experimental situation with finite-difference time domain (FDTD) and we can say that the EM wave propagating in PC behaves like a massive quasi-particle with the $\mathbf{k} \bullet \mathbf{p}$ theorem. A light beam is traveling through different media. As our research progresses, we will look for physics suited to this technology and develop appropriate structures.

Materials with a negative refractive index do not violate the laws of physics according to a series of recent experiments and computer simulations. First proposed in 1968, these materials - which bend light in the opposite direction to conventional materials, and which are also known as left-handed materials - were only demonstrated in experiments for the first time in 2000. However, some physicists argued that although the phase velocity of the light was negatively refracted, the group velocity was not. Others claimed that negative refraction violated causality by permitting velocities greater than the speed of light. Several experiments [6] and simulations

[7] have now demonstrated that negative refraction is real and that causality is not violated.

Recently, the one-dimensional (1D) version of a photonic crystal has long been known as a multilayer reflector, but 2-dimention/3-dimention (2D/3D) photonic crystals have only recently started to attract attention after the appearance of a prediction that photonic insulators can be developed by photonic crystals [10]. In photonic crystals, light travels as Bloch waves, in a similar way to plane waves in continuous material. Bloch waves travel through crystals with a definite propagation direction despite the presence of scattering, but their propagation is complicated because it is influenced by the band structure. There have been some works related to this issue in the literature, but systematic and consistent way of understanding is still lacking. Therefore, we will clarify features of light propagation in photonic crystals, and show how a strongly modulated photonic crystal exhibits remarkably interesting propagation characteristics which can be understood as refractionlike phenomenon in standard geometrical optics with unusual refractive index.

1-3 Organization of the thesis

We will systematically analyze the light propagation phenomena in periodic structures and photonic crystals with the help of the band theory and numerical simulations. Our research is to examine whether light propagation in photonic crystals can be understood by simple geometrical optic analogies. First, we will present the effect of the band folding that is directly related to the periodic boundary condition of the structure. Second, we'll describe the novel phenomenon with microwave experimental frame. And then, we'll discuss the experimental phenomenon with $\mathbf{k} \bullet \mathbf{p}$ theory. It will been shown that the propagation characteristics of diffraction gratings and weakly modulated photonic crystals are much alike and can be explained within a similar framework. This explains anomalous propagation phenomena in photonic crystals. These studies have clarified that the light propagation in these media is fundamentally different from conventional refraction, and therefore we cannot define appropriate refractive index. Then, in order to support our experiment and $\mathbf{k} \bullet \mathbf{p}$ theorem, we will use the FDTD algorism to simulate our experimental setup. We will demonstrate the negative refractive phenomenon.

Chapter 2 Theory and Methodology

2-1 Introduction

2-1.1 Refraction phenomenon in homogenous medium

When light enters a transparent medium it is refracted as shown in FIG. 1. Refraction is the cause of the apparent bending of a ray of light when it enters water or glass. The magnitude of the effect is given by the *index of refraction* or *refractive index*, n, where:

$$n = \sin q_1 / \sin q_2 \tag{2.1}$$

q_1 being called the angle of incidence and q_2 the angle of refraction .this equation is known as Snell's law. The plane of incidence is the plane containing the incident ray and the normal to the surface. The above equation is a special case of the more general relation:

$$\sin q_1 / \sin q_2 = n_2 / n_1 \tag{2.2}$$

for light passing from a medium of refractive index n_1 to one of refractive index n_2.

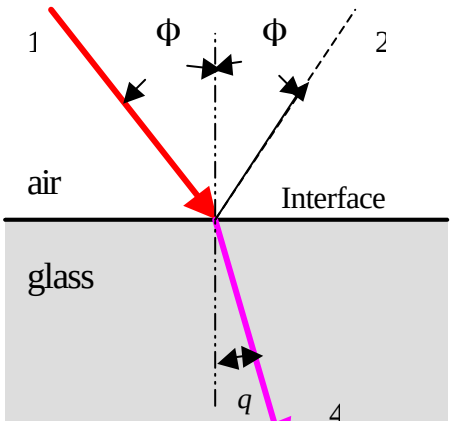

Fig. 1 the light beam appears to bend at the interface by an amount given by Snell's law.

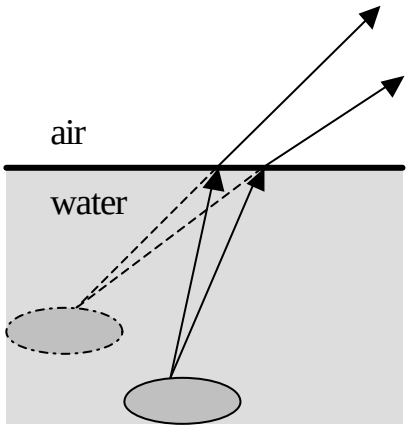

Fig. 2 because of refraction at the air-water. The object be seen to bend upwards

The effect of refraction is familiar to anyone who has looked into a deep pool of water. In a swimming pool, for example, the bottom always seems closer to the surface than it really is. For the same reason, a stick will appear bent towards the surface when dipped into water, as shown in figure kingfishers, birds which catch fish by diving into rivers, must allow for this effect and aim below the object that they apparently see in order to hit the target, as depicted in FIG. 2.

In effect, the refractive index is a manifestation of the fact that the light is slowed down on entering a transparent material. We shall see below that this is due to the interaction of the light with the electrons around the atoms which make up the solid. It is found that the refractive index, n, of a transparent substance is given by:

n = velocity of light in a vacuum (c) / velocity of light in the medium (v)

The frequency of the light does not alter when it enters a transparent medium and because of the relationship between the velocity of a light wave and its frequency:

$$n l = velocity \tag{2.3}$$

it is possible to write:

$$n = c / v = l_{vac} / l_{subs} \tag{2.4}$$

where l_{vac} is the wavelength of the light wave in a vacuum and l_{subs} is the wavelength in the transparent substance. It is thus seen that light has a smaller wavelength in a transparent material than in vacuum.

2-1.2 Refraction phenomenon in photonic crystal

A photonic crystal is a structure whose refractive index is periodically modulated, and the resultant photonic dispersion exhibits a band nature analogous to the electronic band structure in a solid. What is the refraction phenomenon in photonic crystal? Over the last decade, the one-dimensional (1D) version of a photonic crystal has long been known as a multilayer reflector, but 2D/3D photonic crystals have only recently started to attract attention after the appearance of a prediction that photonic insulators can be developed by photonic crystals. In photonic crystals, light travels as Bloch waves, in a similar way to plane waves in continuous material. Bloch waves

travel through crystals with a definite propagation direction despite the presence of scattering, but their propagation is complicated because it is influenced by the band structure. We are interesting in this big problem.

The essential explanation of these phenomena should lie in the photonic band structure because the direction of light propagation inside the photonic crystal is determined by the equifrequency surface of the photonic bands in these structures. This is the most important physics picture what we want to present. Although this feature of photonic crystals has been frequently discussed, there have been very few reports about quantitative comparison between theory and experiment so far. Considering this feature, it might be possible to reconstruct the photonic band structure from measurements of the light propagation inside the photonic crystal. ***S. Kawakami*** ***et al.*** recently demonstrated such an experiment for 3D Si/SiO2 photonic crystals that were fabricated by auto cloning technology and his work was published [11]**.** A very detailed photonic band structure was successfully obtained by the measurement, which was published by **M. Notomi** *et al.* [12]**..** This experiment directly shows that the light propagation is indeed determined by the photonic band structure. This means that, if we want to investigate the light propagation in photonic crystals, what we have to do is just to calculate the corresponding photonic band structure. However, photonic band structures are fairly complicated and it is thus not easy to understand the light propagation phenomena in photonic crystals in qualitative terms. Moreover, the relation between the light propagation in photonic crystals and that in conventional dielectric materials or gratings has yet to be clearly demonstrated. We believe that a simpler way of understanding light propagation in photonic crystals is possible and should be established, which will clarify the difference between behavior in photonic crystals and conventional refraction or diffraction phenomena. As mentioned above, light propagation in photonic crystals is represented by Bloch waves. Bloch waves have a definite propagation direction in spite of strong scattering by the periodic structure. This character leads us to consider a geometrical optic approach to understand the propagation in it. In conventional geometrical optics in dielectric materials, light propagation—as shown in Fig. 3—is described by the phase refractive index and Snell's law. However, the phase velocity is defined as the velocity of the propagation of an equi-phase surface. This velocity has a definite meaning, for example, for plane waves and spherical waves for which the equi-phase surface can be defined without ambiguity, in the

photonic crystal, however, the equi-phase surface cannot be difined rigorously, since its eigenfunction is a superposition of plane waves. This means that the phase velocity cannot be defined appropriately in photonic crystal. Therefore, in order to pursue geometrical approaches for photonic crystals, we will examine the concept of phase refractive index and the group refractive index for photonic crystals. The phase refractive index of photonic crystals has been discussed by several authors in the long wavelength limit. [13-15].They have homogenized the periodic structures and deduced an appropriate phase index in the lowfrequency limit. However, such a result cannot be extended to higher frequencies of which wavelength becomes comparable to, or smaller than, the lattice period. Since most of interesting phenomena, including unusual beam propagation, occur outside the low-frequency limit, we are not satisfied with this homogenization method to understand the light propagation in photonic crystals.

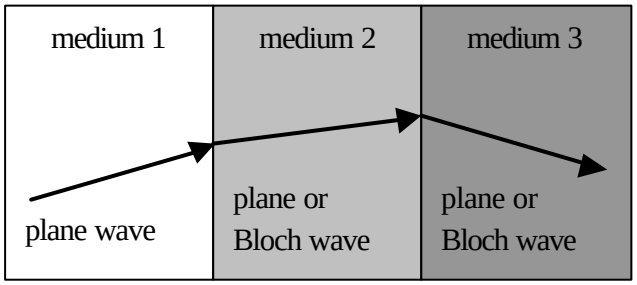

Fig. 3 Schematic diagram of light propagation phenomenon through different media.

About the refraction phenomenon, there are some works to discuss the phase refraction index. Lin *et al*. investigated the lowest band of a 2D photonic crystal near its first gap, and argued that the refractive index is modified from the low-frequency limit value near the gap because the slope of the dispersion curve is reduced[16]. This effect is not significantly large because the control range of index is limited within refractive indices of materials. The present photonic crystal effect simply arises as a modification of the mixing ratio of index values, similar to the way in which the effective refractive index of a conventional slab wave guide is derived.[17] Furthermore, their argument did not show whether the index they deduced could be meaningful outside the low-frequency limit (**M. Notomi** *et al*. showed that such index is

generally meaningless except under a certain condition and it is not clear how this index is related to propagation direction)[7]. Dowling *et al.* used essentially the some argument, which the phase refraction index equation is n=*ck/w*, to predict an ultra small index for photonic crystals.[18] This effect is due to the reduction of wave vector *k* near the zone center as a result of the band folding. However, this argument leads to an ultra small *n* even for an empty lattice with the same crystal structure. In their photonic crystal model, we know that light propagation in such an empty-lattice photonic crystal (at least when its frequency does not satisfy the Bragg condition) should be normal; however, this model still predicts abnormal phase index. This apparent contradiction shows that the deduced small *n* does not posses real meaning and that the band folding itself does not lead to unusual beam propagation. This contradiction arises mainly because we have only considered *k* in the above analysis. We must also consider the group velocity vector to study beam propagation in photonic crystals. We thus need to investigate the equifrequency surface (EFS) of the photonic band structure to discuss the negative refractive phenomenon, and the propagation direction which should be positive or negative could be corresponded to the k.p theorem directly.

We can describe the index of refraction with the EFS of the photonic crystal. Firstly, we show a very simple example of EFS analysis in FIG. 4, which describes a light incident problem from air to a dielectric material. A circle in the figure is an EFS of the photonic band of a dielectric, namely, *v*=*ck/w*. The *k* vector in the dielectric medium is determined by the continuity of tangential components of the *k* vector across the interface, and light always propagates parallel to the *k* vector in this case. This is an EFS expression of conventional refraction phenomenon, and this plot is a graphical representation of Snell's law in *k* space

$$\sin q_1 / \sin q_2 = n_2 / n_1 \tag{2.5}$$

In photonic crystal, the light propagate direction is highly related to the EFS. We can show the reciprocal lattice space to describe the phenomenon In FIG. 4. We can take the FIG. 4 into two part. One is the photonic crystal with the small index modulation, and the other is the PC with the finite index modulation which was larger than former. In the situation, if a plane wave is launched to this photonic crystal from air at a certain incident angle, several phenomena are expected from this figure. First, a light beam is decomposed into more than one nonidentical

waves. In the situation in Fig.4(a), two waves A and B are excited. Wave A corresponds to a transmitted wave, and wave B is a diffracted wave. Second, the propagation direction is apparently not parallel to the k vector for diffracted waves. The propagation direction is oriented to the group velocity vector $\boldsymbol{v}_g = \nabla_k \boldsymbol{W}$ which is normal to the EFS. Third, the propagation angle is very sensitive to the incident angle and wavelength if the launched beam excites the waves near intersecting points (e.g., point C), which leads to large beam steering. This is the origin of the superprism effect as reported in Ref. [6]. Fourth, in some regions of the EFS near the Γ point, k vector becomes very small and it leads to a very small index value. But such an index is not meaningful by the same reason as for a grating. As readers already may have noticed, the situation as a whole is similar to that for a grating. The anomalous beam propagation in photonic crystals can be explained by the mechanism outlined above for a diffraction grating. Consequently, we still cannot define a proper phase refractive index for a weakly modulated photonic crystal which precisely reflects the light propagation. On the other hand, we can know that the photonic band structure is the highly related reason of the negative refraction phenomenon. We will discuss the phenomenon with the k.p theorem and FDTD algorism. Whereas, with the k.p theory, the photons can be viewed as the quasi-particals. We can describe the negative refraction phenomenon as the photons trapped on the interface between photonic crystal medium and air latter.

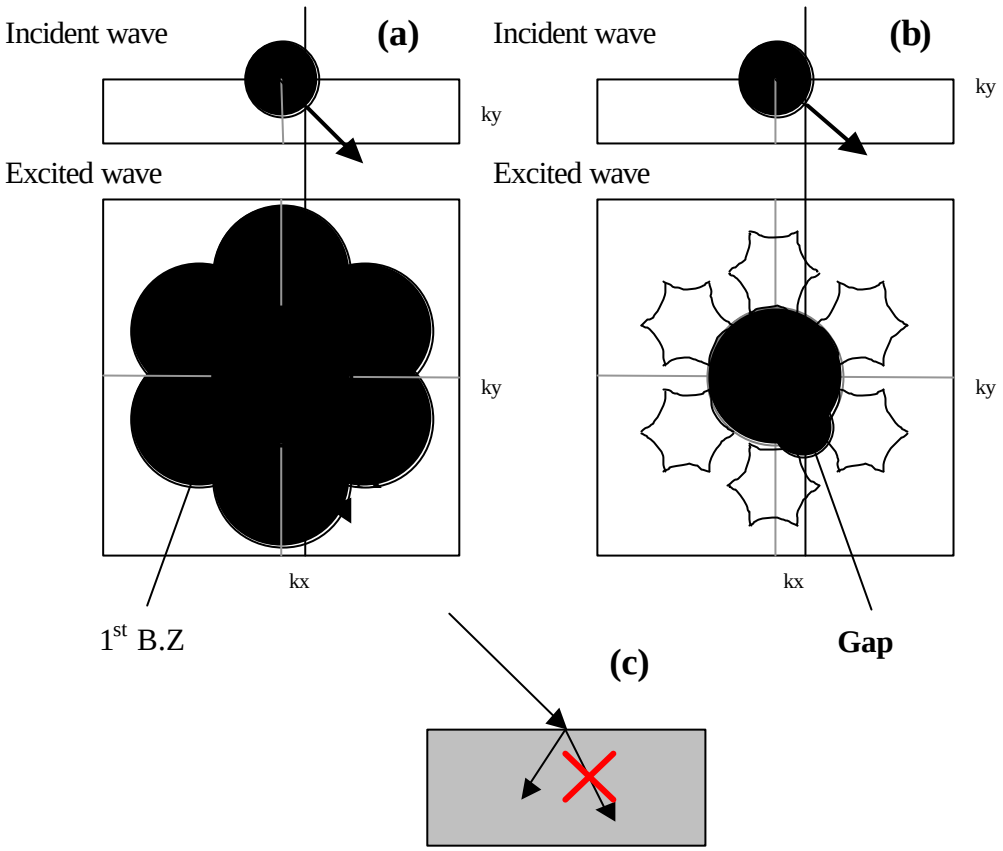

Fig. 4 (a) Schematic EFS plot for a hexagonal 2D photonic crystal with a varnishing small index modulation. The first Brillouin zone (BZ) is shown as a hexagon. (b) EFS plot for a hexagonal 2D photonic crystal with finite index modulation. This type of EFS is general for photonic crystals at frequencies far from the gaps or photonic crystals with a small index modulation. (c) Schematic of anomalous diffraction near the singular point.

2-2 Refractive index in photonic crystal

2-2.1 Phase velocity, Group velocity, and Energy velocity

In photonic crystal, we can use the plane-wave expansion method to calculate the dispersion relations of the radiation modes in the photonic crystals. we can also calculate their wave functions. In addition to the eigenfrequencies and eigenfunctions, there are several parameters that characterize the radiational waves. One of them is the wave velocity. In contrast to the case

of particles for which the velocity has a single meaning, waves have three different kinds of velocities, i.e., the phase velocity, the group velocity, and the energy velocity. These velocities are equal to each other in uniform materials with dielectric constants which are real and independent of frequency.

The phase velocity is defined as the velocity of the propagation of an equi-phase surface. This velocity has a definite meaning, for example, for plane waves and spherical waves for which the equi-phase surface can be defined without ambiguity, in the photonic crystal, however, the equi-phase surface cannot be defined rigorously, since its eigenfunction is a superposition of plane waves. This means that the phase velocity cannot be defined appropriately in photonic crystal.

On the other hand, the group velocity, which is the velocity of the propagation of a wave packet, can be defined as usual:

$$\boldsymbol{v}_g = \frac{\partial w}{\partial \boldsymbol{k}} \tag{2.6}$$

The energy velocity is defined as the velocity of the propagation of the electromagnetic energy. The propagation of the electromagnetic energy is described by Poynting's vector. The time-averaged Poynting's vector $\boldsymbol{S}_{kn}(\boldsymbol{r})$ is given by

$$\begin{aligned} \boldsymbol{S}_{kn}(\boldsymbol{r}) &\equiv average < \mathrm{Re}\left[\boldsymbol{E}_{kn}(\boldsymbol{r})e^{-iw_{kn}t}\right] \times \mathrm{Re}\left[\boldsymbol{H}_{kn}(\boldsymbol{r})e^{-iw_{kn}t}\right] > \\ &= \frac{1}{2}\mathrm{Re}\left[\boldsymbol{E}_{kn}(\boldsymbol{r}) \times \boldsymbol{H}_{kn}^{*}(\boldsymbol{r})\right] \end{aligned} \tag{2.7}$$

On the other hand, the time-averaged electromagnetic energy density $U_{kn}(\boldsymbol{r})$ is given by

$$\begin{aligned} u_{kn}(\boldsymbol{r}) &\equiv \frac{\boldsymbol{e}_0 \boldsymbol{e}(\boldsymbol{r})}{2} average\left\{\left\{\mathrm{Re}\left[\boldsymbol{E}_{kn}(\boldsymbol{r})e^{-iw_{kn}t}\right]\right\}^2\right\} + \frac{\boldsymbol{m}_0}{2} average\left\{\left\{\mathrm{Re}\left[\boldsymbol{H}_{kn}(\boldsymbol{r})e^{-iw_{kn}t}\right]\right\}^2\right\} \\ &= \frac{1}{4}\left\{\boldsymbol{e}_0 \boldsymbol{e}(\boldsymbol{r})\left|\boldsymbol{E}_{kn}(\boldsymbol{r})\right|^2 + \boldsymbol{m}_0\left|\boldsymbol{H}_{kn}(\boldsymbol{r})\right|^2\right\} \end{aligned} \tag{2.8}$$

Thus, the energy velocity $\boldsymbol{v}_e$ is defined as

$$\boldsymbol{v}_e = \frac{\left\langle \boldsymbol{S}_{kn}(\boldsymbol{r})\right\rangle}{\left\langle \boldsymbol{u}_{kn}(\boldsymbol{r})\right\rangle} \tag{2.9}$$

Where $\langle \cdots \rangle$ means the spatial average.

Now, the group velocity is equal to the energy velocity even though the dielectric constant is modulated periodically. The proof was given by Yeh[19].

$$\boldsymbol{v}_e = \boldsymbol{v}_g \tag{2.10}$$

2-2.2 Calculation of Group Velocity

As we learned in the last section, the group velocity of the radiation modes has very important role in light propagation and optical response in the photonic crystals. Hence, the calculation of the group velocity is an essential task for the understanding of their optical properties. Since the group velocity is defined as the derivative of the angular frequency with respect to the wave vector, we may calculate it by numerical differentiation. That is, we may actually evaluate the following limit:

$$\boldsymbol{v}_g = \lim_{\Delta \boldsymbol{k} \to 0} \frac{w_{\boldsymbol{k}+\Delta k,n} - w_{\boldsymbol{k},n}}{\Delta \boldsymbol{k}} \tag{2.11}$$

This numerical differentiation needs a limiting procedure for which we have to know a series of eigenfrequencies as a function of the wave vector.

There is quite a convenient method to avoid this procedure and give an accurate evaluation of the group velocity. We use the Hellmann-Feynman theorem for this purpose, with which the readers may be familiar as it relates to quantum mechanical calculations. In the case of quantum mechanics, the Hellmann-Feynman theorem is stated as follows. First, we assume an Hermitian operator $\hat{H}$ that depends on an external variable a, and denote it by $\hat{H}_a$. We also assume that we know the orthonormal set composed of the eigenfunctions of $\hat{H}_a$, which we denote by $\{|an\rangle; n = 1,2,\Lambda\}$:

$$\begin{aligned} &\hat{H}_a |an\rangle = l_{an} |an\rangle, \\ &\langle an|an\rangle = 1 \end{aligned} \tag{2.12}$$

In the above two equations, we used the standard notation of "bra" and "ket" vectors. l_{an} is the eigenvalue of $\hat{H}_a$ for state $|an\rangle$ and $\langle\Lambda|\Lambda\rangle$ denotes the inner product. Now, our problem is to calculate the derivative of l_{an} with respect to a. Because the state vector (or the eigenfunction) $|an\rangle$ is normalized to unity, the following.holds.

$$\begin{aligned}\frac{\partial}{\partial a} l_{an} &= \frac{\partial}{\partial a}\langle an|\hat{H}_a|an\rangle \\ &= \frac{\partial\langle an|}{\partial a}\hat{H}_a|an\rangle + \langle an\left|\frac{\partial\hat{H}_a}{\partial a}\right|an\rangle + \langle an|\hat{H}_a\frac{\partial|an\rangle}{\partial a} \\ &= l_{an}\frac{\partial}{\partial a}\langle an|an\rangle + \langle an\left|\frac{\partial\hat{H}_a}{\partial a}\right|an\rangle \\ &= \langle an\left|\frac{\partial\hat{H}_a}{\partial a}\right|an\rangle .\end{aligned} \tag{2.13}$$

Once we know the analytical expression of $\partial\hat{H}_a/\partial a, \partial l_{an}/\partial a$ can readily be obtained using this equation without the limiting procedure in (2.11).

Now, we will see how to use the Hellmann-Feynman theorem for the calculation of the group velocity. Here, we show the method for the E polarization. The dispersion relation is obtained by solving the eigenvalue equation, which is the photonic band structure correspond to.

When we define a column vector $\boldsymbol{A}_{\boldsymbol{k}//n}$ by

$$\boldsymbol{A}_{\boldsymbol{k}//n}(\boldsymbol{G}_{//}) = |\boldsymbol{k}_{//} + \boldsymbol{G}_{//}|E_{z,\boldsymbol{k}//n}(\boldsymbol{G}_{//}), \tag{2.14}$$

When we apply Bolch's theorem to structure the plane-wave method, we obtain the following eigenvalue equations for the expansion coefficients in E-polarization condition:

$$\sum_{\boldsymbol{G}'_{//}} k\left(\boldsymbol{G}_{//} - \boldsymbol{G}'_{//}\right)\left|\boldsymbol{k}_{//} + \boldsymbol{G}'_{//}\right|^2 E_{z,\boldsymbol{k}_{//}n}(\boldsymbol{G}'_{//}) = \frac{w^{(E)^2}_{\boldsymbol{k}_{//}n}}{c^2} E_{z,\boldsymbol{k}_{//}n}(\boldsymbol{G}_{//}), \tag{2.15}$$

is transformed to

$$M_{k_{//}}\boldsymbol{A}_{\boldsymbol{k}_{//}n} = \frac{w^{(E)^2}_{kn}}{c^2}\boldsymbol{A}_{\boldsymbol{k}_{//}n}, \tag{2.16}$$

where $M_{\boldsymbol{k}_{//}}$ is a $\boldsymbol{k}_{//}$-dependent matrix whose $(\boldsymbol{G}_{//}, \boldsymbol{G}_{//}^{'})$component is given by the following equation:

$$\boldsymbol{M}_{\boldsymbol{k}_{//}}(\boldsymbol{G}_{//}, \boldsymbol{G}_{//}^{'}) = |\boldsymbol{k}_{//} + \boldsymbol{G}_{//}||\boldsymbol{k}_{//} + \boldsymbol{G}_{//}^{'}|k(\boldsymbol{G}_{//} - \boldsymbol{G}_{//}^{'}). \tag{2.17}$$

The $\boldsymbol{k}_{//}$-dependent vector $\boldsymbol{A}_{k_{//}n}$ gives the engenfunction $\boldsymbol{E}_{z,k_{//}n}(\boldsymbol{r}_{//})$ as

$$E_{z,\boldsymbol{k}_{//}n}(\boldsymbol{r}_{//}) = h\sum_{G_{//}} \frac{A_{k_{//}n}(\boldsymbol{G}_{//})}{|\boldsymbol{k}_{//} + \boldsymbol{G}_{//}|}\exp\{i(\boldsymbol{k}_{//} + \boldsymbol{G}_{//}) \cdot \boldsymbol{r}_{//}\}, \tag{2.18}$$

and it is normalized to unity, i.e., $|\boldsymbol{A}_{k_{//}n}| = 1$,h is the normalization constant.

Here, we assume that $e(\boldsymbol{r}_{//})$ is real. Then, $k(-\boldsymbol{G}_{//}) = k^{*}(\boldsymbol{G}_{//})$ and $M_{k_{//}}$ is an Hermitian matrix. Therefore, we can apply the Hellmann-Feynman theorem to the present problem, and we obtain

$$\boldsymbol{A}_{k_{//}n}^{t*}\frac{\partial M_{k_{//}}}{\partial k_{//}}\boldsymbol{A}_{k_{//}n} = \frac{\partial}{\partial \boldsymbol{k}_{//}}\left(\frac{w_{k_{//}n}^{(E)^2}}{c^2}\right) = \frac{2w_{k_{//}n}^{(E)}}{c^2}\frac{\partial w_{k_{//}n}^{(E)}}{\partial \boldsymbol{k}_{//}}, \tag{2.19}$$

where t denotes the transposed matrix and

$$\frac{\partial M_{\boldsymbol{k}_{//}}(\boldsymbol{G}_{//}, \boldsymbol{G}_{//}^{'})}{\partial \boldsymbol{k}_{//}} = \left\{\frac{|\boldsymbol{k}_{//} + \boldsymbol{G}_{//}^{'}|}{|\boldsymbol{k}_{//} + \boldsymbol{G}_{//}|}(\boldsymbol{k}_{//} + \boldsymbol{G}_{//}) + \frac{|\boldsymbol{k}_{//} + \boldsymbol{G}_{//}|}{|\boldsymbol{k}_{//} + \boldsymbol{G}_{//}^{'}|}(\boldsymbol{k}_{//} + \boldsymbol{G}_{//}^{'})\right\}k(\boldsymbol{G}_{//} - \boldsymbol{G}_{//}^{'}) \tag{2.20}$$

Therefore, the group velocity $v_g(w, n)$ can be readily evaluated once the eigenvector $\boldsymbol{A}_{k_{//}n}$ and the eigenvalue $w_{k_{//}n}^{(E)^2}/c^2$ are obtained by the band calculation based on the plane-wave expansion method.

2-3 Electromagnetic simulation using the FDTD method

2-3.1 Introductions to the FDTD algorism

In 1966 Yee [20] proposed a technique to solve Maxwell's curl equations using the finite-difference time-domain (FDTD) technique. Yee's method has been used to solve numerous scattering problems on microwave circuits, dielectrics, and electromagnetic absorption in biological tissue at microwave frequencies [21-26].

Initially there was little interest in the FDTD method, probably due to a lack of sufficient computing resources [26]. However, with the advent of low cost, powerful computers and advances to the method itself, the FDTD technique has become a popular method for solving electromagnetics problems, especially in periodic structure.

2-3.2 One dimension free space formulation

The time-dependent Maxwell's curl equations in free space are

$$\begin{aligned}\frac{\partial \boldsymbol{E}}{\partial t} &= \frac{1}{\boldsymbol{e}_0}\nabla \times \boldsymbol{H} \\ \frac{\partial \boldsymbol{H}}{\partial t} &= -\frac{1}{\boldsymbol{m}_0}\nabla \times \boldsymbol{E}\end{aligned} \tag{2.21}$$

E and H are vectors in three dimensions, so in general, Eq.(2.21) represent three equations each. We will star with a simple one-dimensional case using only E_x and H_y, so Eq.(2.21) become

$$\begin{aligned}\frac{\partial E_x}{\partial t} &= -\frac{1}{\boldsymbol{e}_0}\frac{\partial H_y}{\partial z} \\ \frac{\partial H_y}{\partial t} &= -\frac{1}{\boldsymbol{m}_0}\frac{\partial E_x}{\partial z}.\end{aligned} \tag{2.22}$$

There are the equations of a plane wave with the electric field oriented in the x direction, magnetic field oriented in the y direction, and traveling in the z direction.

Taking the central difference approximations for both the temporal and spatial derivatives gives

$$\begin{aligned}\frac{E_x^{n+1/2}(k) - E_x^{n-1/2}(k)}{\Delta t} &= -\frac{1}{\boldsymbol{e}_0}\frac{H_y^n(k+1/2) - H_y^n(k-1/2)}{\Delta x} \\ \frac{H_y^{n+1}(k+1/2) - H_y^n(k+1/2)}{\Delta t} &= -\frac{1}{\boldsymbol{m}_0}\frac{E_x^{n+1/2}(k+1) - E_x^{n+1/2}(k)}{\Delta x}\end{aligned} \tag{2.23}$$

in these two equations, time is specified by the superscripts, i.e., "n" actually means a time $t = \Delta t \cdot n$. Remember, we have to discrete everything for formulation into the computer. The term "*n+1*" means one time step later. The terms in parentheses represent distance, i.e., "*k*" actually means the distance $z = \Delta x \cdot k$. (However, Δx is so commonly used for a spatial increment that I will use Δx.)The formulation of Eq. (2.23) assumes that the $\boldsymbol{E}$ and $\boldsymbol{H}$ fields are interleaved in both

space and time. $\boldsymbol{H}$ uses the argument k+1/2 and k-1/2 to indicate that the $\boldsymbol{H}$ field values are assumed to be located between the E field values.

Let us return to discuss the stability. An electromagnetic wave propagating in free space cannot go faster than the speed of light. So the relationship between Δx and Δt can be written as the well-known "Courant Condition"

$$\Delta t \le \frac{\Delta x}{\sqrt{n}c} \tag{2.24}$$

where n is the dimension of the simulation and c is the speed of light.

We still need to add incident wave source condition and absorbing boundary condition. It is a great subject in talking about the wave source condition. For simplicity, we divide it into two categories: hard source and soft source. In a hard source, a propagation wave will see that value and be reflected, because the hard value of E_x looks like a metal wall to FDTD. However a soft source is added to E_x at a certain point and a propagating pulse will just pass through. In calculating photonic crystal, we must consider the field scattering from the boundary. Therefore we use a soft source. And, in order to support our experimental result we use the plane wave incident as our source. We will introduce the periodic structure simulation with FDTD method further.

2-3.3 Simulation in periodic structure

In order to simulate a photonic crystal medium, we have to add the relative dielectric constant $\boldsymbol{e}_r$ to Maxell's equations:

$$\begin{aligned} \frac{\partial \vec{\boldsymbol{E}}}{\partial t} &= \frac{1}{\boldsymbol{e}_r \boldsymbol{e}_0} \nabla \times \vec{\boldsymbol{H}} \\ \frac{\partial \vec{\boldsymbol{H}}}{\partial t} &= -\frac{1}{\boldsymbol{m}_0} \nabla \times \vec{\boldsymbol{E}} \end{aligned} \tag{2.25}$$

In PC medium, the dielectric constant $\boldsymbol{e}_r$ is periodic.

We have been using the form of Maxwell's equations, which use only the $\boldsymbol{E}$ and $\boldsymbol{H}$ files. We

will begin by normalizing these equations, using

$$\tilde{\boldsymbol{E}} = \sqrt{\frac{e_0}{m_0}} \cdot \boldsymbol{E}$$
$$\tilde{\boldsymbol{D}} = \sqrt{\frac{1}{e_0 \cdot m_0}} \cdot \boldsymbol{D}, \tag{2.26}$$

which leads to

$$\frac{\partial \tilde{\boldsymbol{D}}}{\partial t} = \frac{1}{\sqrt{e_0 m_0}} \nabla \times \tilde{\boldsymbol{H}}$$
$$\tilde{\boldsymbol{D}}(w) = e_r^*(w) \cdot \tilde{\boldsymbol{E}}(w) \tag{2.27}$$
$$\frac{\partial \tilde{\boldsymbol{H}}}{\partial t} = -\frac{1}{\sqrt{e_0 m_0}} \nabla \times \tilde{\boldsymbol{E}}$$

where $\boldsymbol{D}$ is the electric flux density. Notice that Eq.(2.27) is written in the frequency domain.

We will assume we are dealing with a lossy dielectric medium of the form

$$e_r^*(w) = e_r + \frac{s}{jwe_0} \tag{2.28}$$

and substitute Eq.(2.28) into (2.27):

$$\boldsymbol{D}(w) = e_r \cdot \boldsymbol{E}(w) + \frac{s}{jwe_0} \boldsymbol{E}(w). \tag{2.29}$$

taking the first term into the time domain is not a problem because it is simple multiplication. In the second term, Fourier theory tells us that $1/jw$ in the frequency domain is integration in the time domain, so Eq.(2.29) becomes

$$\boldsymbol{D}(t) = e_r \cdot \boldsymbol{E}(t) + \frac{s}{e_0} \int_0^t \boldsymbol{E}(t') \cdot dt' \tag{2.30}$$

we will want to go to the sampled time domain, so the integral will be approximated as a summation over the time steps Δt

$$\boldsymbol{D}^n = e_r \cdot \boldsymbol{E}^n + \frac{s \cdot \Delta t}{e_0} \sum_{i=0}^{n} \boldsymbol{E}^i = e_r \cdot \boldsymbol{E}^n + \frac{s \cdot \Delta t}{e_0} \boldsymbol{E}^n + \frac{s \cdot \Delta t}{e_0} \sum_{i=0}^{n-1} \boldsymbol{E}^i \tag{2.31}$$

now we can calculate $\boldsymbol{E}^n$

$$\boldsymbol{E}^{n} = \frac{\boldsymbol{D}^{n} - \frac{s \cdot \Delta t}{e_0} \sum_{i=0}^{n-1} \boldsymbol{E}^{i}}{e_r + \frac{s \cdot \Delta t}{e_0}} \tag{2.32}$$

Suppose now that we are asked to calculate the E field distribution at every point in a dielectric medium subject to illumination at various frequencies. One approach would be to use a sinusoidal source and iterate the FDTD program until we observe that a steady state has been reached, and determine the resulting amplitude and phase at every point of interest in the medium. This would work, but then we must repeat the process for every frequency of interest. System theory tells us that we can get the response to every frequency if we use an impulse as the source. We could go back to using the Gaussian pulse, which, if it is narrow enough, is a good approximation to an impulse, which, if it is narrow enough, is a good approximation to an impulse. We then iterate the FDTD program until the pulse has died out, and take the Fourier transform of the E fields in the slab. If we have the Fourier transform of the E field at a point, then we know the amplitude and phase of the E field that would result from illumination by any sinusoidal source. This, too, has a very serious drawback: the E field for all the time domain data at every point of interest would have to be stored until the FDTD program is through iteration so the Fourier transform of the data could be taken, presumably using a fast Fourier transform algorithm. This presents a logistical nightmare.

Here is an alternative. Suppose we want to calculate the Fourier transform of the E field $\boldsymbol{E}(t)$ at a frequency f_1. This can be done by the equation

$$E(f_1) = \int_0^{t_T} E(t) \cdot e^{-j2\pi f_1 t} dt. \tag{2.33}$$

Notice that the lower limit of the integral is 0 because the FDTD program assumes all causal functions. The upper limit is t_T, the time at which the FDTD iteration is halted. Rewriting (2.33) in a finite difference form.

$$E(f_1) = \sum_{n=0}^{T} E(n\Delta t) e^{-j2\pi f_1 (n\Delta t)} \tag{2.34}$$

Where T is the number of iterations and Δt is the time step, so $t_T = T \cdot \Delta t$. Equation (2.34) may be divided into its real and imaginary parts

$$E(f_1) = \sum_{n=0}^{T} E(n \cdot \Delta t) \cdot \cos(2pf_1 \cdot \Delta t \cdot n) - j \sum_{n=0}^{T} E(n \cdot \Delta t) \cdot \sin(2pf_1 \cdot \Delta t \cdot n). \qquad (2.35)$$

Note that there is an amplitude and phase associated with every frequency at each cell.

In our simulation, I use it to observe the plane wave propagate through the photonic crystal prism. We can not only get the phase distribution with every frequency at our simulation domain of our question but find the amplitude distribution.

However, absorbing boundary conditions (ABCs) are necessary to keep outgoing $\boldsymbol{E}$ and $\boldsymbol{H}$ fields form being reflected back into the problem space. Normally, in calculating the $\boldsymbol{E}$ field, we need to know the surrounding $\boldsymbol{H}$ values; this is a fundamental assumption of the FDTD method. At the edge of the problem space we will not have the value to one side. However, we have an advantage because we know there are no sources outside the problem space. Therefore, the fields at the edge must be propagating outward. We will use these two facts to estimate the value at the end.

One of the most flexible and efficient ABCs is the perfectly matched layer (PML) developed by Berenger [27]. In our simulation problem, we use this way to prevent the boundary refraction of the propagation light. Whereas, in order to simulate a plane wave in a 2D FDTD program, the problem space will be divided up into two regions, the total field and the scattered field (FIG. 5). There are two primary reasons for doing this: (1) The propagation plane wave should not interact with the absorbing boundary conditions; (2) the load on the absorbing boundary conditions should be minimized. These boundary conditions are not perfect, i.e., a certain portion of the impinging wave is reflected back into the problem space. By subtraction the incident field, the amount of the radiation field hitting the boundary is minimized, thereby reducing the amount of error.

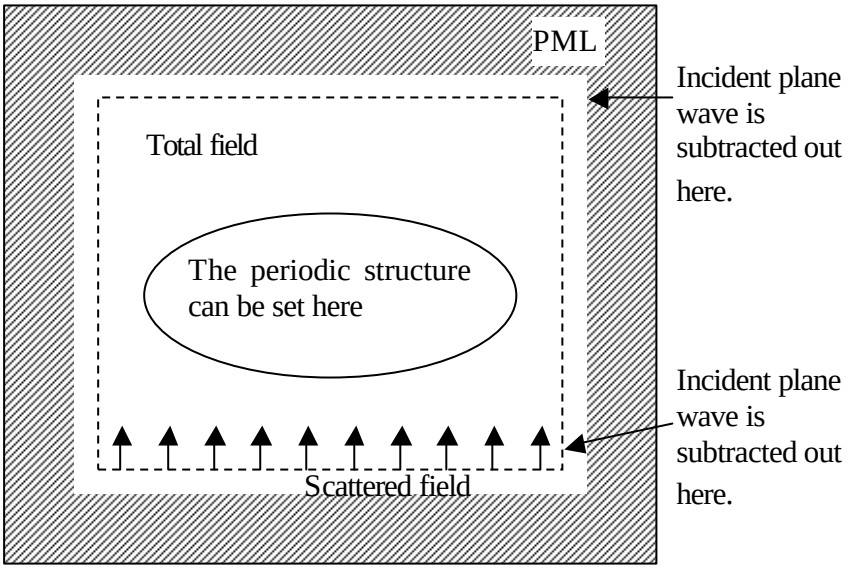

Fig. 5 Total field/scattered field of the two-dimensional problem space

2-4 k • p theory

In order to study the propagation of light in a photonic crystal, we start from the Maxwell's equations in cgs units:

$$\nabla \cdot \vec{B} = 0, \qquad \nabla \times \vec{E} + \frac{1}{c}\frac{\partial \vec{B}}{\partial t} = 0,$$
$$\nabla \cdot \vec{D} = 4\pi\rho, \qquad \nabla \times \vec{H} - \frac{1}{c}\frac{\partial \vec{D}}{\partial t} = \frac{4\pi}{c}\vec{J}, \tag{2.36}$$

where **E** and **H** are the macroscopic electric and magnetic fields, **D** and **B** are the displacement and magnetic induction fields, and ρ and **J** are the free charge and current densities. We consider the light propagation within a periodic mixed dielectric medium, a composite of regions of homogeneous dielectric material, with no free charge or currents (ρ =**J**=0).

In general, the components D_i of the displacement field **D** are related to the component E_i of the electric filed **E** via a complicated power series. First we assume the field strengths are small

enough so that we are in the linear regime, or the operation frequency region far away from the resonance frequency region of the photonic materials. Second, we assume the medium is macroscopic and isotropic, so that **E**(**r**,w) and **D**(**r**,w) are related by a scalar dielectric constant e(**r**,w). Third, we ignore any explicit frequency dependence of the dielectric constant and treat e(**r**) as purely real, i.e., the materials which construct the photonic crystals are non-dispersive.

$$\vec{D}(r) = e(r)\vec{E}(r) \tag{2.37}$$

For most dielectric materials of interest, the magnetic permeability is very close to unity and we may set **B** = **H**. Then, we can assume the fields that happen to vary harmonically with time, so that we have

$$\begin{aligned} \vec{H}(r,t) &= \vec{H}(r)e^{iwt} \\ \vec{E}(r,t) &= \vec{E}(r)e^{iwt} \end{aligned} \quad . \tag{2.38}$$

Because there is no free charge or current, the electromagnetic waves considered to be transverse. When we eliminate (2.38) in (2.36), we obtain the following equations:

$$\Theta_E \vec{E}(r) \equiv \frac{1}{e(r)}\nabla\times\{\nabla\times\vec{E}(r)\} = \frac{w^2}{c^2}\vec{E}(r), \tag{2.39}$$

$$\Theta_H \vec{H}(r) \equiv \nabla\times\{\frac{1}{e(r)}\nabla\times\vec{H}(r)\} = \frac{w^2}{c^2}\vec{H}(r). \tag{2.40}$$

Solving (2.39) and (2.40) are the eigen-value problems, the eigen-values construct the photonic crystal structure.

One of the most important techniques for investigating the properties of a function is the study of its power series expansion. Now we introduce the new basis as follows:

$$\mathbf{H}(\mathrm{r}) = \sum_{np} A_n(\mathbf{k}) H_{np}(\mathbf{k}_0, r)\exp(-iS\cdot r) \quad , \tag{2.41}$$

$\mathbf{S}$=k-k_0 ,

where $\mathbf{k}$ is a wave vector lies within the first Brillouin zone, and $\mathbf{k}_0$ is a specific wave-vector in which the band maximum or minimum occurs with S= |**S** |<<1 near the band edge and $A_n(\mathbf{k})$ being the expansion coefficients. $\mathbf{H}_{n,p}$ ($\mathbf{k_0}$, **r**) are the Bloch-type eigenfunctions of eq.(2.40) belong $\mathbf{k_0}$ wave vector and the corresponding eigenvalues are $\omega_n(\mathbf{k_0})$ which can be derived by plane-wave expansion method, where n is a band index and p represents the index of physical

solutions ($\omega_n(\mathbf{k_0}) \neq 0$) and unphysical solutions ($\omega_n(\mathbf{k_0}) = 0$). If we define

$$c_n(\mathbf{k}, r) \equiv H_{np}(\mathbf{k}_0, r)\exp(-iS \cdot r)\,. \tag{2.42}$$

The properties of orthonormality and completeness can be easily proofed that

$$\int c_n^*(q,r)\, c_m(k,r)dr = d_{nm}d(k-q)\,,$$

$$\sum_n \int c_n^*(k,r)\, c_n(k,r')dk = d(r-r')\,. \tag{2.43}$$

$c_n(\mathbf{k}, r)$ also obeys Bloch's theorem for a state vector $\boldsymbol{k}$

$$c_n(\mathbf{k}, r+a) = \exp(ik\cdot a)\, c_n(\mathbf{k}, r)\,, \tag{2.44}$$

where $\boldsymbol{a}$ is lattice constant. An equation for the $A_n(\mathbf{k})$ is determined by substituting eq. (2.42) into eq. (2.40):

$$\begin{aligned}
&\vec{P}\times[\frac{1}{\vec{e}(r)}\vec{P}\times\vec{c}_n(k,r)] \\
&= \exp(i(\vec{k}-\vec{k}_0)\cdot\vec{r})\{\hbar(\vec{k}-\vec{k}_0)\times[\frac{\hbar(\vec{k}-\vec{k}_0)}{\vec{e}(r)}\times H_{np}(\mathbf{k}_0,r)] \\
&\quad + \vec{P}\times[\frac{\hbar(\vec{k}-\vec{k}_0)}{\vec{e}(r)}\times H_{np}(\mathbf{k}_0,r)] + \hbar(\vec{k}-\vec{k}_0)\times[\frac{\vec{P}}{\vec{e}(r)}\times H_{np}(\mathbf{k}_0,r)] \\
&\quad - E_n(\vec{k}_0)H_{np}(\mathbf{k}_0,r)\}
\end{aligned}\,, \tag{2.45}$$

where $\vec{P} \equiv -i\hbar\vec{\nabla}$, $E \equiv (\hbar w/c)^2$ and eq.(2.45) can be rewritten as

$$\vec{P}\times(\frac{1}{\vec{e}(r)}\vec{P}\times\vec{c}_n(k,r)) + E(\vec{k})\vec{c}_n(k,r) = 0\,. \tag{2.46}$$

If $\vec{k}_0$ is the extreme of the band

$$\frac{dE_n(\vec{k})}{dk^r}|_{\vec{k}=\vec{k}_0} = 0 \tag{2.47}$$

with making the unitary transformation $H_n = \exp[iS]h_n$ in which **S**=k-k_0 is a Hermitian operator, we have derived an effective dielectric tensor equation that has a similar structure of the effective-mass equation in semiconductors an can be written as

$$(\frac{1}{e^*})_{ab} \equiv \frac{1}{2\hbar^2}\frac{\partial^2 E_n(\vec{k}_0)}{\partial k^a \partial k^b}\,. \tag{2.48}$$

Using the effective-dielectric tensor of eq. (2.48), the Hermitian (2.47) can written as an

eigenvalue equation

$$E_n(\mathbf{k})A_n(\mathbf{k}) = [E_n(\mathbf{k}_0) + \sum_{ab} \hbar^2 (\frac{1}{e})_{ab} S^a S^b]A_n(\mathbf{k}) . \tag{2.49}$$

Eq. (2.49) is the well-known effective-mass equation, written, however, in momentum space. To get more useful formulation, we introduce an envelope function

$$F_n(r) = \int e^{iS\mathbf{g}r} A_n(\mathbf{k}) d^3k \tag{2.50}$$

the integration being over the first Brillouin zone . Thus, we have

$$(\frac{\hbar w_n}{c})^2 F_n(\mathbf{r}) = [(\frac{\hbar w_n(\mathbf{k}_0)}{c})^2 + \sum_{ab} \hbar^2 (\frac{1}{e})_{ab} \frac{\partial}{\partial x_a}\frac{\partial}{\partial x_b}]F_n(\mathbf{r}), \tag{2.51}$$

where i and j are indices of three different directions of **r** . We can also transform eq. (2.51) back to the time space to study the temporal evolution of $F(\mathbf{r}, t)$. We have a tensor equation:

$$\frac{\partial^2}{\partial t^2} F_n(\mathbf{r}, t) = [(\frac{\hbar w_n(\mathbf{k}_0)}{c})^2 + \sum_{ab} \hbar^2 (\frac{1}{e})_{ab} \frac{\partial}{\partial x_a}\frac{\partial}{\partial x_b}]F_n(\mathbf{r}, t) . \tag{2.52}$$

Eq. (2.52) is equivalent to the Maxwell equation of eq. (2.40), under the $\mathbf{k} \bullet \mathbf{p}$ theory, which is the generalized Klein-Gordon equation and is reduced to the Klein-Gordon equation in isotropic medium. This equation indicates there is an energy-storing mechanism near band edges, thus we have defined $m_h = \eta\omega_n(\mathbf{k}_0)/c^2$ as the inertial mass of quasi-particle(QP) of photon. The inertial mass m_h is dependent on the band index n and is quantized. Although, by assuming the band mixing is negligible, we applied the one-band $\mathbf{k} \bullet \mathbf{p}$ theory to study photons near band edges.

To understand the negative refraction phenomena, we shall use the extended $\mathbf{k} \bullet \mathbf{p}$ theory, proposed by Johnson *et al.* [28], i.e., K.P theory provides an approximate approach to study the phenomenon of the light traveling in the PCs. The practical usefulness of K.P method is that these K.P parameter can be obtained by fitting either to band structure of bulk PCs calculated using computationally intensive methods to EM waves propagating in PC.

According to the extended $\mathbf{k} \bullet \mathbf{p}$ theory, we can describe the negative refraction phenomenon in photonic crystal. The physical modle to describe the phenomenon will be shown exhaustively in chapter four.

Chapter 3 Experiment

3-1 Experimental setup

Our 2D isosceles right triangular PCP, which consists of a square lattice of alumina rods (dielectric constant e = 8.9 and diameter of 4.0 mm) surrounded by air, is shown in Fig. 8. The square lattice supported by two polystyrene plates has lattice constant 15.0 mm. The length of rods is 14.0 cm and is long enough to be considered infinitely long in a reasonable approximation, especially in the high frequency region, if the propagation direction is perpendicular to the rods. The microwave is incident perpendicularly to the one of the right-angle sides as shown in Fig. 6. Therefore, the forward direction of the microwave makes a 45^o with respect to the normal of the bevel of PCP, which is the exit interface of PC and air. The experiment setup [as shown in Fig. 7] was supported by the polystyrene bulk 1.0 m above the ground to prevent the background noise disturbing the transmission signal. The bulk PC or PCP was placed behind a rectangular aperture of a metal shield and two horn antennas were connected to a HP 8720A network analyzer to measure the transmission power of microwave passing through the bulk PC and PCP. Because an EM waveform horn antenna creates spherical wave front, we have set the emitter antenna far away from the tested sample, in order to make the incident wave on the sample having planar wave front. The incident microwaves were transverse magnetic (TM) waves, where the direction of electric fields is parallel to the axis of the rods.

In order to measure the refraction angles from the exit interface of PCP, the receiving antenna was attached to a pivot right on top of the PCP. For every frequency within 11.5 to 18 GHz, the receiver horn was rotated by 1.875^o per step. The indices of refraction for different frequencies were then deduced from measured refraction angles.

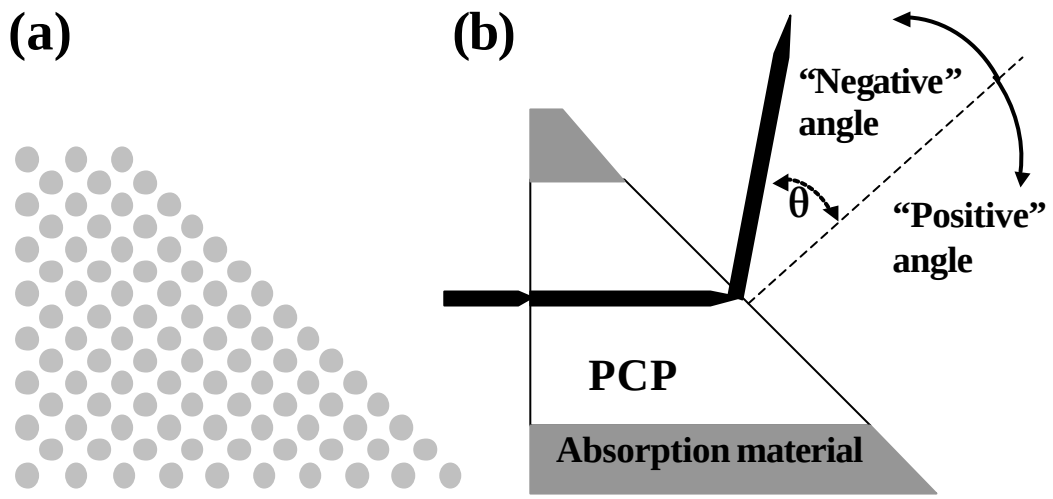

Fig. 6 (a) a 2D isosceles right triangle photonic crystal prism (PCP); and (b) the schematics of an incident EM wave passing through PCP.

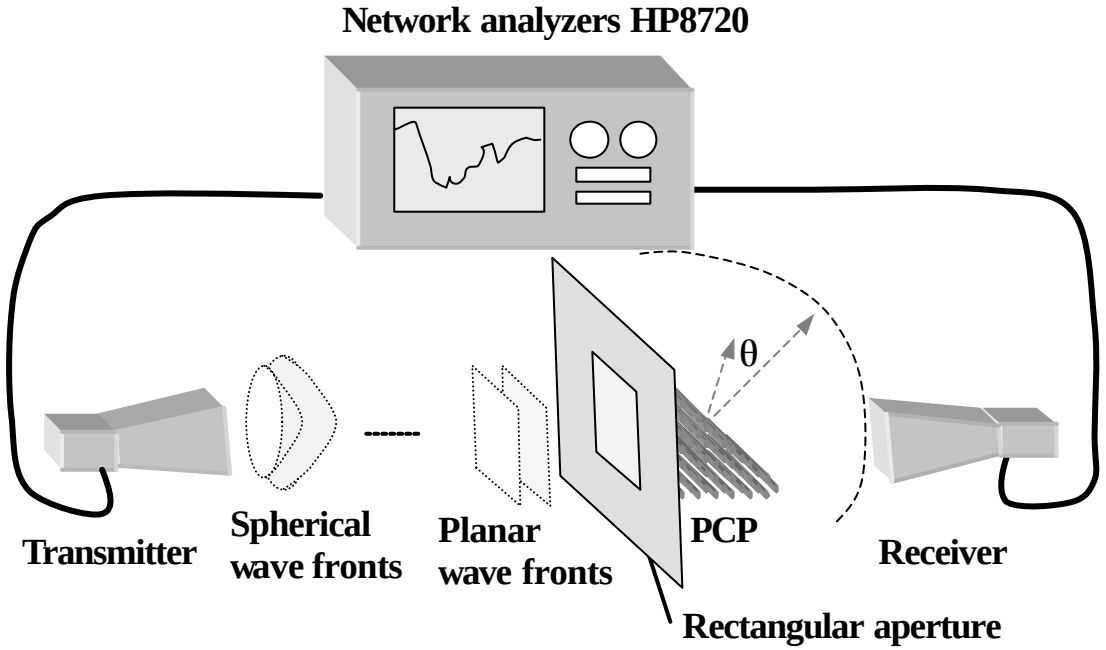

Fig. 7 The experiment setup of measuring microwave transmission of a photonic crystal.

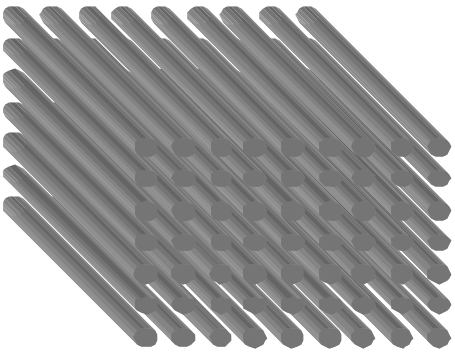

Fig. 8 Photonic crystal

- The 2D photonic crystals in this study consist of alumina rods forming a square lattice. The rods are supported on both sides by polystyrene plate.
- The 4.00-mm diameter alumina rods, making up the square lattice having a lattice constant of 15.00mm, have a dielectric constant of 8.9 and are surrounded by air.
- For PC structure, the rods are long enough (14cm) to be considered infinitely long to a reasonable approximation, especially in high frequency regions, if the propagation direction is perpendicular to the rods.

- **HP 8720 Microwave Network Analyzer**

The HP 8720 is a high performance microwave network analyzer for measurements of reflection and transmission parameters. It covers the frequency range of 130 MHz to 20 GHz with 1 Hz frequency resolution. It integrates a synthesized source, a switching S-parameter test set, and a duel channel receiver to measure and display magnitude, phase, and group delay of transmitted and reflected power. Time domain provides the capability of transforming measured data from the frequency domain to the time domain. We use it to measure the transmittance phenomenon in photonic crystal in microwave regime.

Chapter 4 Results and Discussion

4-1 The photonic crystal sample measurement

In Fig. 9, we show the photonic band structure, calculated by plane-wave expansion [29], of TM modes of a square PC lattice and the measured transmission spectrum of bulk PC along Γ to M direction. The transmission spectrum is consistent with the calculated band structure in which the photonic-band gap lies within 7.5 to 11.5 GHz. The lowest band exists below 7.5 GHz, where shows very extremely noisy.

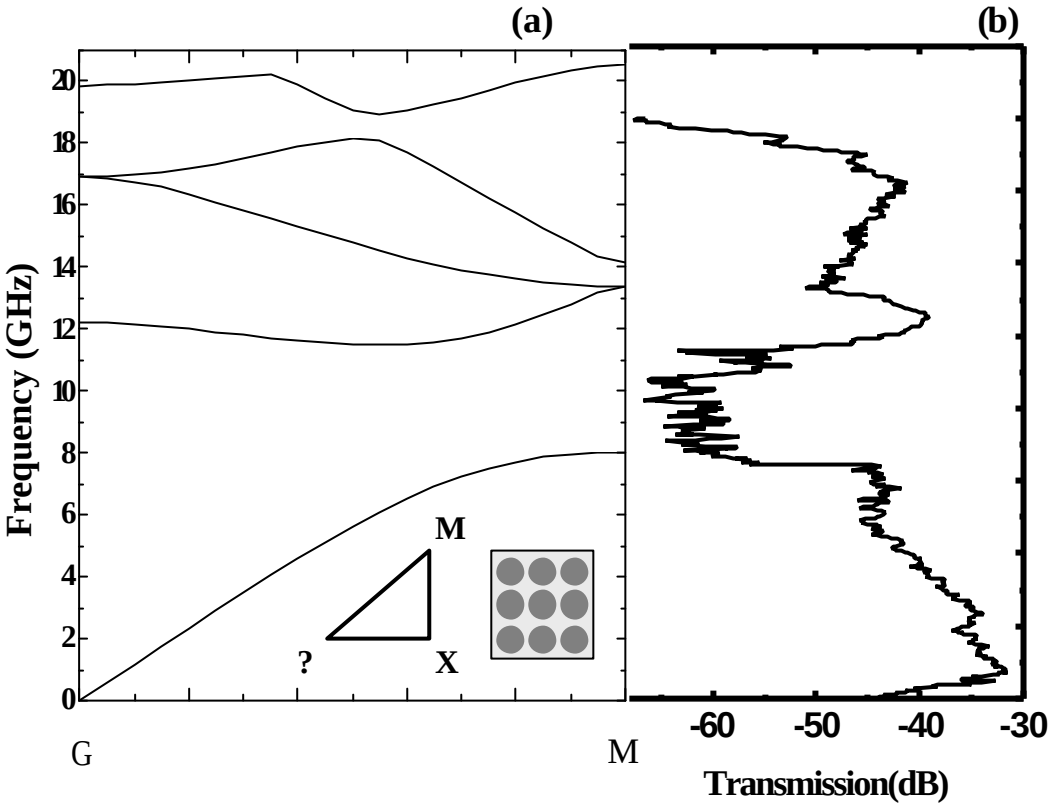

Fig. 9 The photonic band structure (a) of the square PC for the TM polarization, calculated by plane-wave expansion method, and the measured transmission spectrum (b) of bulk PC along Γ to M direction. The transmission spectrum is consistent with the calculated band structure in which the photonic-band gap lies between 7.5 to 11.5 GHz.

4-2 The refraction angle measurement

Because the third and fourth bands, existing between 11.5 GHz and 18.0 GHz, show much less noise, our experiment was performed within this frequency range. In order to measure the refraction angles from the exit interface of PCP, the receiving antenna was attached to a pivot right on top of the PCP. For every frequency within 11.5 to 18 GHz, the receiver horn was rotated by 1.875^{o} per step. The indices of refraction for different frequencies were then deduced from measured refraction angles.

Shown in Fig. 10(a) are the curves of typical angle-dependent transmission power with

(dotted curve) and without (solid curve) a PCP at 14.5 GHz. Note that a positive refraction angle with respect to the normal of the bevel of PCP is defined for the ordinary refraction [see Fig. 6]. There is a very small transmission at negative angles as the EM wave propagates directly through the aperture without PCP. We found that the transmission power in the presence of the PCP is larger than that of free space at certain negative refraction angles. However, there are still some microwaves transmit directly without refraction due to finite width of PCP. The transmittance is then evaluated by taking the ratio of transmitted powers with and without the PCP as shown in Fig. 10(b). There are two peaks located at refraction angles of $-33^0 \pm 3^0$ and $-58^0 \pm 3^0$, respectively. Since the incident beam makes an angle of 45^o with the normal of exit interface of the PCP, we used the Snell's law and obtained two corresponding refraction indices as $n = -0.77$ and -0.22 at 14.5 GHz. In fact, we observed two sets of negative indices of refraction in the frequency range of 14.0 to 18.0 GHz. shown in Fig.11 are angular dependent transmission with (solid curves) and without (dotted curves) at the different incident microwave frequencies. All of them reveal negative refraction.

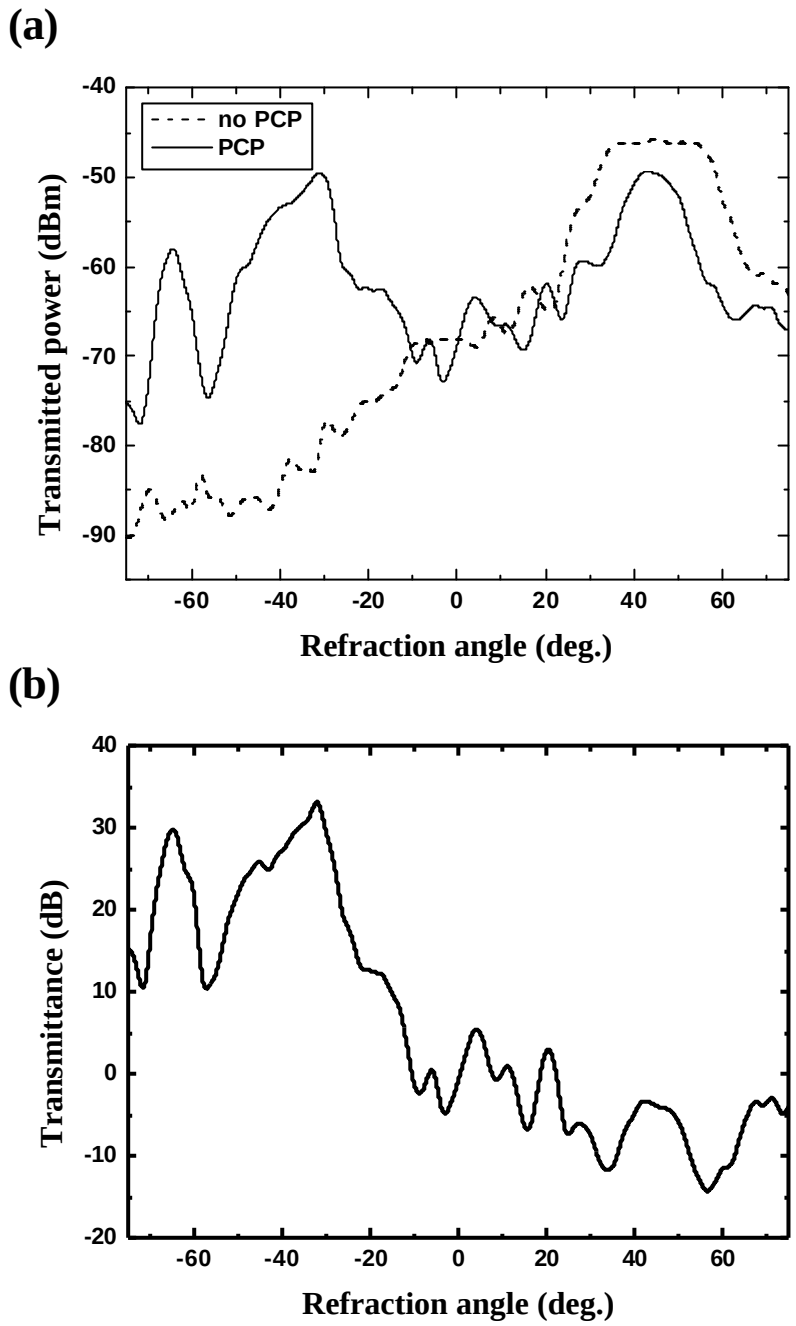

Fig. 10 (a) A typical angle-dependent transmission power with (dotted curve) and without (solid curve) a PCP at 14.5 GHz; and (b) the transmittance is evaluated by the ratio of transmitted powers with and without the PCP.

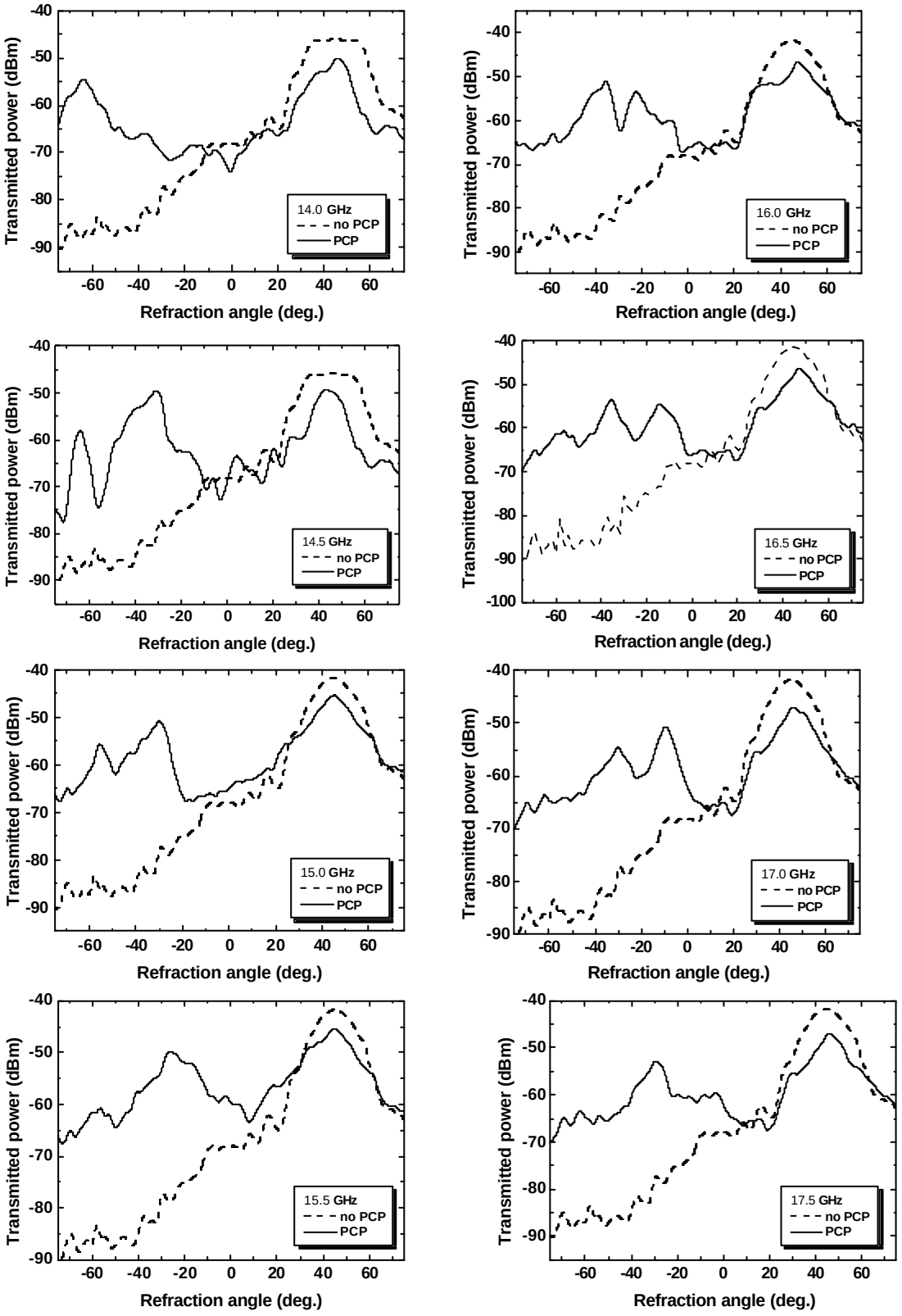

Fig. 11 Angle-dependent transmission with (solid curve) and without (dotted curve) a PCP at 14 GHz, at various incident microwave frequencies as labeled.

4-3 The negative refraction index discussed in k•p theory

To understand the negative refraction phenomena, we shall use the extended **k • p** theory, proposed by Johnson *et al.* [28], to EM waves propagating in PC. According to the extended **k • p** theory, we can define the reciprocal effective-dielectric tensor for the nth band [30]:

$$\frac{1}{e^{n}_{ab}} = \frac{1}{2c^2}\frac{\partial^2 \left(w_n^2(\mathbf{k})\right)}{\partial k^a \partial k^b}, \tag{4.1}$$

where a, b are indices of three different directions of position **r**, c is the light velocity, **k** is a wave vector lies within the first Brillouin zone. $w_n^2(\mathbf{k})/c^2$ is the corresponding eigenvalue of wave (Hamiltonian) equation with band index n at **k** and $\omega_n(\mathbf{k})$ is the angular frequency of band n at **k**. From the effective-dielectric equation [30], we obtain a generalized dispersion relation of EM waves propagating in PC:

$$\frac{w_n^2(\mathbf{k})}{c^2} = \frac{w_n^2(\mathbf{k}_0)}{c^2} + \sum_{a,b}\left(\frac{1}{e^{n}_{ab}} s_a\ s_b + 2d_{ab}\ p_n^a\ s_b\right), \tag{4.2}$$

where $\mathbf{s} = \mathbf{k} - \mathbf{k}_0$ is the deviation from the wavevector $\mathbf{k}_0$, d_{ab} is the Kronecker delta. $\mathbf{p}_n$ is a band parameter around $\mathbf{k}_0$ given by Johnson *et al* [28] and it behaves like the momentum of quasi-particle, **p,** of the **k • p** term in the electronic problem. Notice that the generalized dispersion relation represents the eigenvalue of wave equation as a function of **k** rather than the (conventional) dispersion relation which expresses the relationship of $\omega_n(\mathbf{k})$. The parameter $\mathbf{p}_n$ is equivalent to the slope of generalized dispersion curve and can be determined by fitting the curve pier wisely.

By performing gradient of (4.2) with respect to **s** (or **k**) and then dividing it by $|k|$, we obtain the group velocity $\mathbf{v}_g = \nabla_s w_n(\mathbf{k})$ at an arbitrary wave vector **k** follow the relation.

$$\frac{w_n(\mathbf{k})}{k}\mathbf{e}_s \cdot \nabla_s w_n(\mathbf{k}) = \frac{c^2(\mathbf{p}_n \cdot \mathbf{e}_s)}{k}, \tag{4.3}$$

where $\mathbf{e}_s$ is the unit vector of **s**. If we define the phase velocity for the Bloch wave of wave vector **k** as $\mathbf{v}_p = \frac{w_n(\mathbf{k})}{k}\mathbf{e}_s$, then

$$\mathbf{v}_p \cdot \mathbf{v}_g = \frac{c^2(\mathbf{p}_n \cdot \hat{\mathbf{e}}_s)}{k} \quad . \tag{4.4}$$

From the Eq. (4.4), if the slope of the generalized dispersion curve along the **s** direction is negative, i.e., $\mathbf{p}_n \cdot \hat{\mathbf{e}}_s < 0$, then $\mathbf{v}_p \cdot \mathbf{v}_g < 0$ represents the negative refraction phenomenon with anti-parallel of phase velocity and group velocity. If we further define the phase index l_p^n and the group index l_g^n of Bloch wave for band *n* as the usual way, i.e., $c / l_{p,g}^n$, we have

$$l_p^n l_g^n = \frac{k}{\mathbf{p}_n \cdot \hat{\mathbf{e}}_s} \tag{4.5}$$

In the negative refraction medium, the phase velocity and the group velocity is anti-parallel to each other, one is not able to tell which way is the forward direction since the wave vector has been folded into the first Brilluoin zone through translation symmetry. Therefore, strictly speaking, only the product of phase index and group index has the physical meaning, thus the phase index and the group index are inseparable. The product is negative in this medium and one can not determine which one of them is negative.

After simple mathematical manipulation of Eq. (4.2), the local optimum $w_{0n}^2(\mathbf{k})/c^2$ is related to the rest mass of the quasi particle by, $m_{0n} = w_{0n}(\mathbf{k})/c^2$ with Planck constant, $\eta = 1$, and the dispersion relation relative to the local optimum can be written as [30]

$$e_n^2 \frac{w^2(\mathbf{k})}{c^2} = e_n^2 m_n^2 c^4 = e_n^2 m_{0n}^2 c^4 + (e_n \mathbf{p}_n)^2 c^2 , \tag{4.6}$$

with $\varepsilon_n \mathbf{p}_n$ being the momentum of the quasi particle. By using Eq. (4.3), we found the group velocity can be defined as the ratio of momentum to relativistic effective mass $m_n^* = \varepsilon_n m_n$ of the quasi-particle, i.e. $v_g = e_n P_n / e_n m_n = c^2 P_n / w_0$. Therefore, we can say that the EM wave propagating in PC behaves like a massive quasi-particle [30].

We show the calculated $l_p^n l_g^n$ of the third and fourth bands along Γ to M direction according to Eq. (4.5) by using the photonic band structure of Fig. 9(a) and compare with the measured negative indices of refraction in Fig. 12 in the frequency range of 13.5 to 18 GHz where two bands, i.e. the third and fourth bands exist. Because both bands are concave

downward, we found $\mathbf{p}_3 \bullet \mathbf{e}_s$ is negative between 13.5 GHz and 17 GHz and $\mathbf{p}_4 \bullet \mathbf{e}_s < 0$ between 14 GHz and 18 GHz. The solid-circle data in Fig. 12 correspond to the dispersion curve of the third band (dashed curve) and the open-square data is a result of the fourth band (dash-dotted curve). We found the theoretically calculated negative group indices of both bands are consistent reasonably well with the experimental data except for those data on the high frequency side of the fourth band. By consulting the band structure, the maximum of the fourth band is a result of two non-crossing bands coupling to each other, therefore, the one-band model of the Eq. (4.2) may not be adequate and two-band model is needed to describe this problem. Form the above discussion, implies that the product of phase index of the Bloch wave and the group index $l_p^n l_g^n$ is equivalent to the refractive index of the photonic crystal.

We have also tried to calculate the group index by performing the gradient of the dispersion relation, i.e., $\nabla_{\mathbf{k}} w_n(\mathbf{k})$ and realized that the group index approaches negative infinity if the frequency is close to the optima and is much larger than the experimental results. The results are showed in Fig.13 . It shows the calculated group indices are too large as compared with the experimental data. These experimental results do not match with the experimental results.

We have observed the electromagnetic waves undergo negative refraction in a two-dimensional photonic crystal prism in microwave frequency regime. By measuring the refraction angles of EM waves propagating through a PCP, and applying the Snell's law to the exit interface of PC and air, we deduced the negative refractive indices. The group index, calculated by taking gradient of the dispersion relation curve, disagrees with the experiment. Whereas, we show that only the product of phase index and group index has the physical meaning. The calculated product of phase index and group index derived from the extended $\mathbf{k} \bullet \mathbf{p}$ theory fit reasonably well with the experimental data.

Thus, it is possible to reconstruct the photonic band structure from measurement of refraction angles for light propagation through the PC. And, according to the extended $\mathbf{k} \bullet \mathbf{p}$ theory, the group velocity of EM waves in PC can be defined as the ratio of momentum to relativistic effect mass of a quasi-particle. The EM wave propagating in PC behaves like a

massive quasi-particle.

With the Hellmann-Feynman theorem which we have discussed in 2-2.2, the refractive index can be readily evaluated once the eigenvector $\boldsymbol{A}_{k_{//}n}$ and the eigenvalue $w_{k_{//}n}^{(E)^2} / c^2$ are obtained by the band calculation based on the plane-wave expansion method.

$$\boldsymbol{A}_k^{t*} \frac{\partial M_k}{\partial k} \boldsymbol{A}_k = \frac{\partial}{\partial k}\left(\frac{w^{(E)^2}}{c^2}\right) = \frac{2w^{(E)}}{c^2}\frac{\partial w^{(E)}}{\partial k}, \tag{4.7}$$

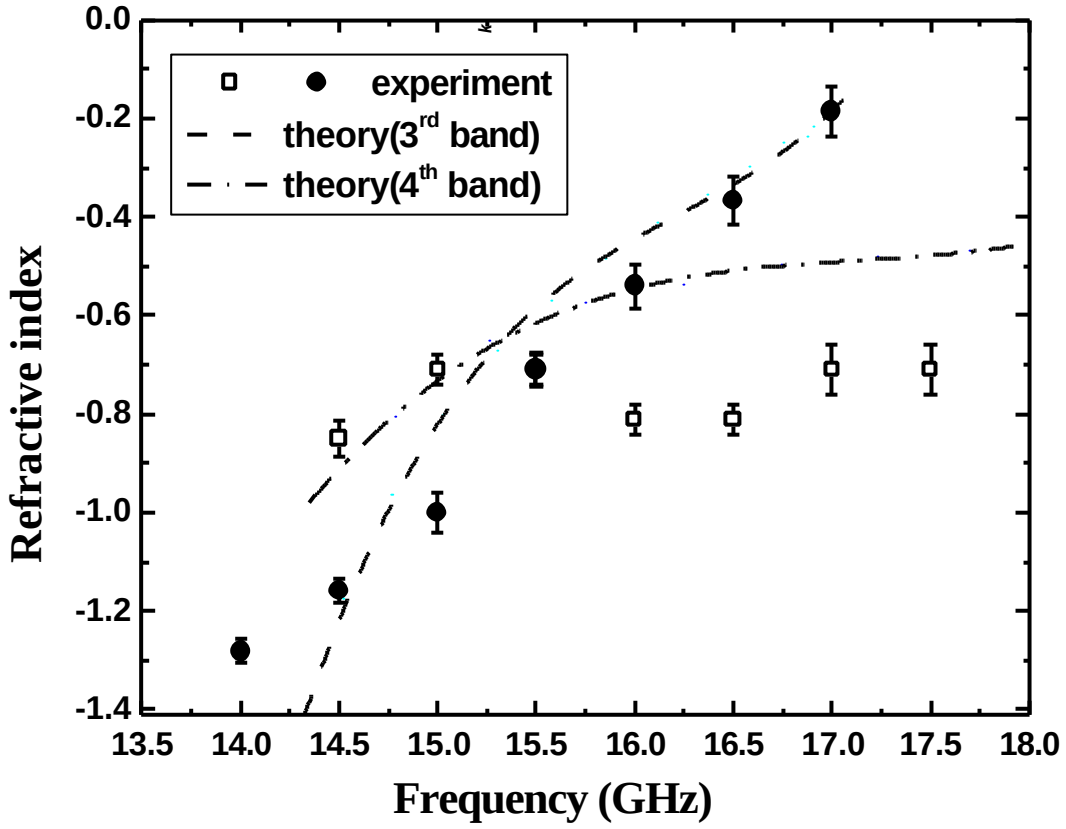

Fig. 12 Comparison between the experimental group indices (solid circles and open squares) and the theoretical group indices with the k.p theorem (the dashed curve and the dash-dotted curve). The group indices of the dashed and the dash-dotted curves are calculated by the dispersion curves of the third and the fourth bands of **Fig. 9**, respectively.

In order to consider the band folding effect, we product the $1/k_o$ into eq.(4.7) , we can get the following form:

$$\frac{1}{k}\frac{\partial}{\partial k}\left(\frac{w_k^{(E)^2}}{c^2}\right) = v_p \cdot v_g \tag{4.8}$$

The eq.(4.8) is equal to the production between group velocity and phase velocity. As the production is negative, the negative refractive phenomenon will be observed. The result can be shown as the Fig. 14. These results have been considered with the band folding.

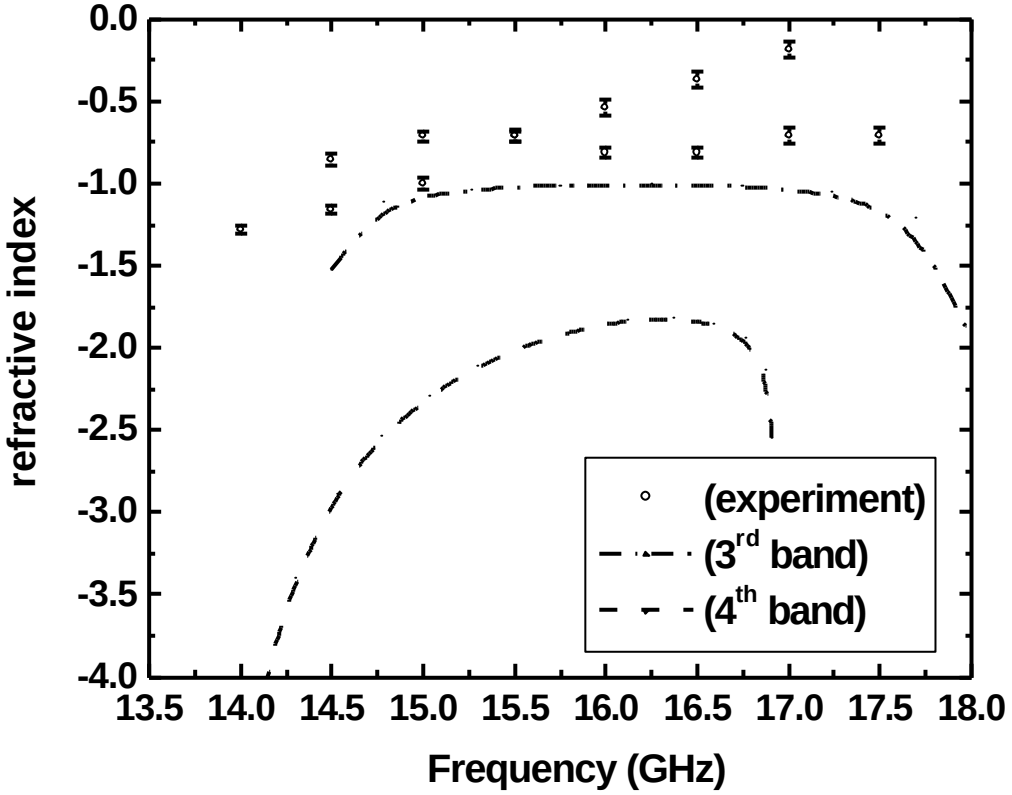

Fig. 13. It shows the calculated group indices are too large as compared with the experimental data.

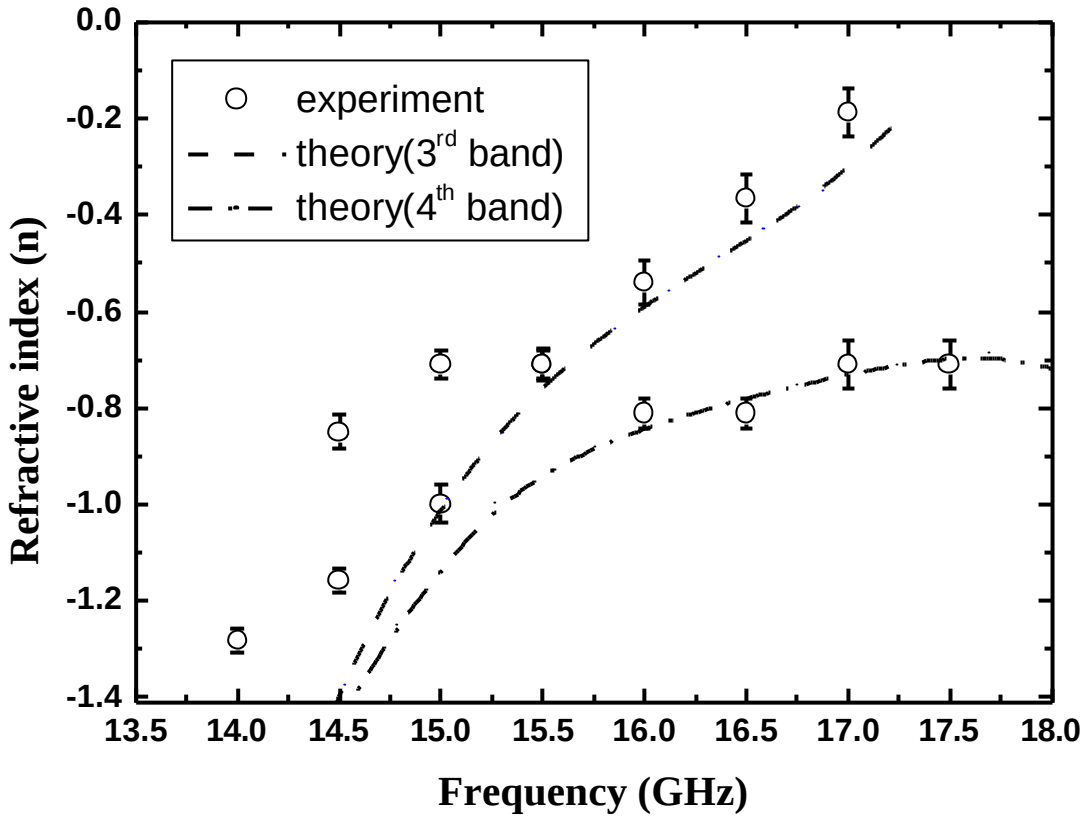

Fig. 14 Comparison between the experimental group indices (solid circles and open squares) and the theoretical group indices with the Hellmann-Feynman theorem (the dashed curve and the dash-dotted curve). The group indices of the dashed and the dash-dotted curves are calculated by the dispersion curves of the third and the fourth bands of **Fig. 9**, respectively.

4-4 The negative refraction phenomenon simulated with the FDTD method

In order to conform the relation of Eq. (4.5), we use the FDTD method to study the refraction phenomenon in material. As plane waves in a nonconductioin medium the phase velocity of the wave is $v = \frac{w}{k} = \frac{1}{\sqrt{me}} = \frac{c}{n}$. The light propagation form can be described with phase velocity directly. This is the conventional refraction phenomenon. The Fig. 15 is shown the EM wave propagation through the glass prism. We can find the normal refraction angle various from different refractive index of glass. So, I can find the light cannot propagate through the glass prism. Because the glass prism and air are all isotropic medium, the propagation of EM wave can be defined as the normal direction of the phase wave front directly. The amplitude distributions can rightly display the refraction phenomenon also. When the index is $\sqrt{2}$, the all-refractive angle is 45^0. This is to be what we show. Other conditions, including the refractive index are 1.2 & 1.3, are displayed.

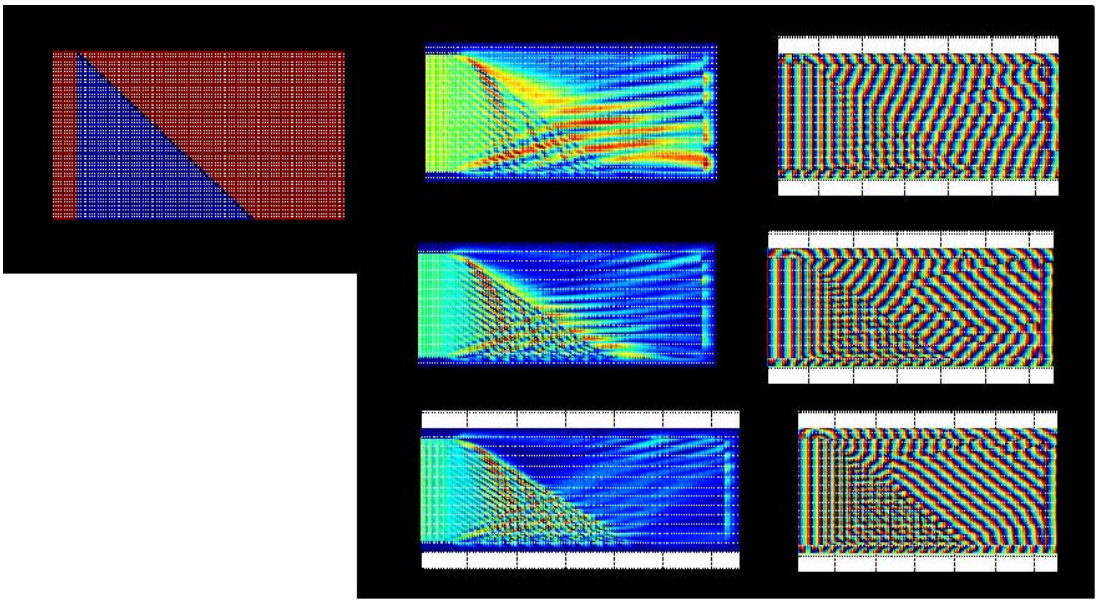

Fig. 15 The EM wave propagates through the glass prism. The refractive phenomenon are shown as the refractive index are 1.2, 1.3, and 1.414. When the index is $\sqrt{2}$, the all-refractive angle is 45^0.

We know the phase velocity is shown as the velocity of the propagation of an equi-phase surface. This velocity has a definite meaning, for example, for plane waves and spherical waves for which the equi-phase surface can be defined without ambiguity. In the photonic crystal, however, the equi-phase surface cannot be defined rigorously, since its eigenfunction is a superposition of plane waves. This means that the phase velocity cannot be defined appropriately in the photonic crystal. As to former, the light propagates with the block wave form in the periodic structure; the refraction index cannot be described with the former EM wave theory all. The phase velocity and group velocity, the both of all, directly involves the refraction phenomenon.

We observe the negative refraction phenomenon with the experiment result already as the EM wave propagate through the photonic crystal prism in negative index state. Now, we use the FDTD algorithm to simulate this phenomenon.

In order to understand our former experimental result that the light propagation in photonic crystals is due to highly anisotropic dispersion surfaces derived by photonic band structure, we have numerically analyzed experiment of a negative index of refraction that the EM wave is refracted by the photonic crystal prism with the finite-difference time domain (FDTD) algorisms [20]. In this simulation, we focus on the structure as shown in the experimental setup. The structure with the photonic crystal prism as our experimental setup is modeled and performed FDTD numerical simulations with perfectly matched layer boundary regions. We show that EM waves, in a frequency range of microwave, undergo negative refraction in a two-dimensional (2D) prism-shaped PC, a photonic crystal prism (PCP). From the refraction angles of EM waves propagating through a PCP, we deduced the indices of negative refraction according to the Snell's law. We choice a plane wave as the incident source, because the wave propagate incident the PCP former plat was planar wave fronts in our real experimental situation. The results are shown in Fig. 16 and Fig. 17 that shows wave fronts with fixed frequency in phase space. It is clear that the incident E-polarized EM wave was refracted by the photonic crystal prism. As to the phase velocity, we use the FDTD method in phase space to find out the phase wave fronts through the photonic structure.

The Fig. 16 show that the plan wave incident the PCP and the discussion surrounding are in the phase domain. The phase wave fronts were refracted with the interface between the air and the photonic crystal. We can use the wave fronts to define the phase refractive index. The phase refraction phenomenon was deduced form the phase velocity which differs from anisotropic and isotropic medium. In our simulation, we can find the refraction differ form varies wavelengths. The negative refraction phenomenon in our simulation problem can correspond to the photonic band structure. It occurs as the fixed frequency in the negative state band. However, the fixed frequency in the three and fourth band regime exist two modes, phase wave fronts display the singularity point. With the Snell's law we defined the refractive index directly. The Fig. 16 show the refractive angle is -18^0 at 16GHz. In the forward direction, we can still find there is the EM wave propagation also. However, the plane wave run through the photonic crystal prism was refracted to the negative angle. In fact, the phase distribution in our discussion domain can be defined as the phase refraction index explicitly. With the Snell's law, we can get the phase refraction index. The direct direction was the phenomenon of the Fourier transform form real space to phase space of the FDTD, even if the propagation amplitude in direct direction is not significant.

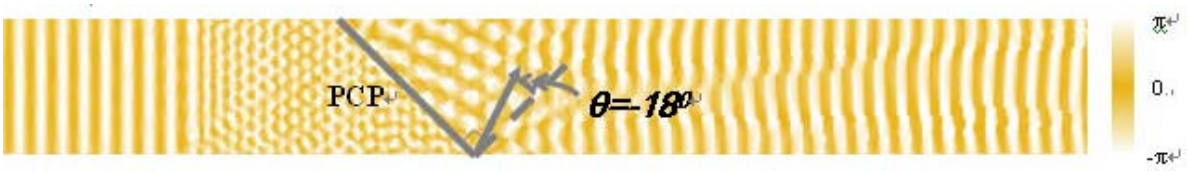

Fig. 16 This shows the refractive angle is -18^0 at 16GHz

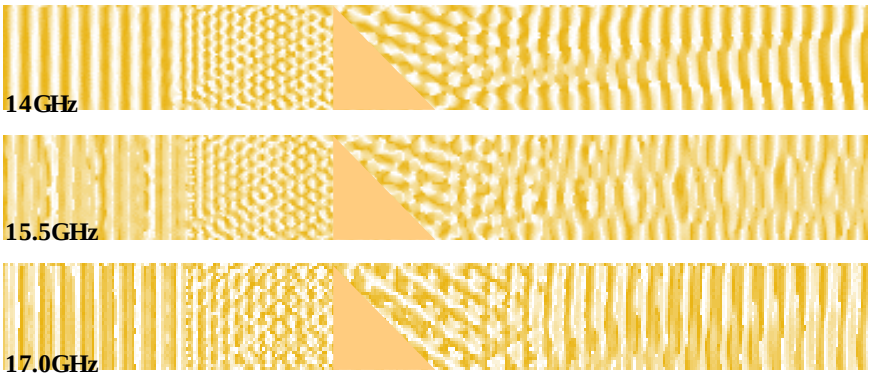

Fig. 17 This shows the refractive angle is different form the different wavelengths

In the negative refraction medium, the phase velocity and the group velocity is anti-parallel to each other, one is not able to tell which way is the forward direction since the wave vector has been folded into the first Brilluoin zone through translation symmetry. Therefore, strictly speaking, only the product of phase index and group index has the physical meaning, thus the phase index and the group index are inseparable. The product is negative in this medium and one can not determine which one of them is negative. By consulting the band structure, the maximum of the fourth band is a result of two non-crossing bands coupling to each other, therefore, the one-band model may be not adequate and two-band model is needed to describe this problem. It implies that the product of phase index of the Bloch wave and the group index $l_p^n l_g^n$ is equivalent to the refractive index of the photonic crystal. It implies that the product of phase index of the Bloch wave and the group index $l_p^n l_g^n$ is equivalent to the refractive index of the photonic crystal.

If we define the phase velocity for the Bloch wave of wave vector $\mathbf{k}$ as $\mathbf{v}_\mathrm{p} = \frac{w_n(\mathbf{k})}{k}\mathbf{e}_s$ and the group velocity as $\mathbf{v}_\mathrm{g} = \nabla_s w_n(\mathbf{k})$, the phase velocity and the group velocity produced to each other is the same to the dispersion relationship of the $\mathbf{k}\bullet\mathbf{p}$ theorem. The form of $l_p^n l_g^n$ is considered the folding effect of the periodic structure. This physical equation includes the wave vector folding to the first Brilluoin zone. That is must be considered at the photonic band structure. We can directly describe the light beam propagate thorough the negative refraction medium with this form.

The **Fig. 19** shows the $l_p^n l_g^n$ match to the experiment data. Although the two refracted mode propagation in the medium, the phase front was not clearly defined. We still can find the experiment data was corresponded to mixed mode well.

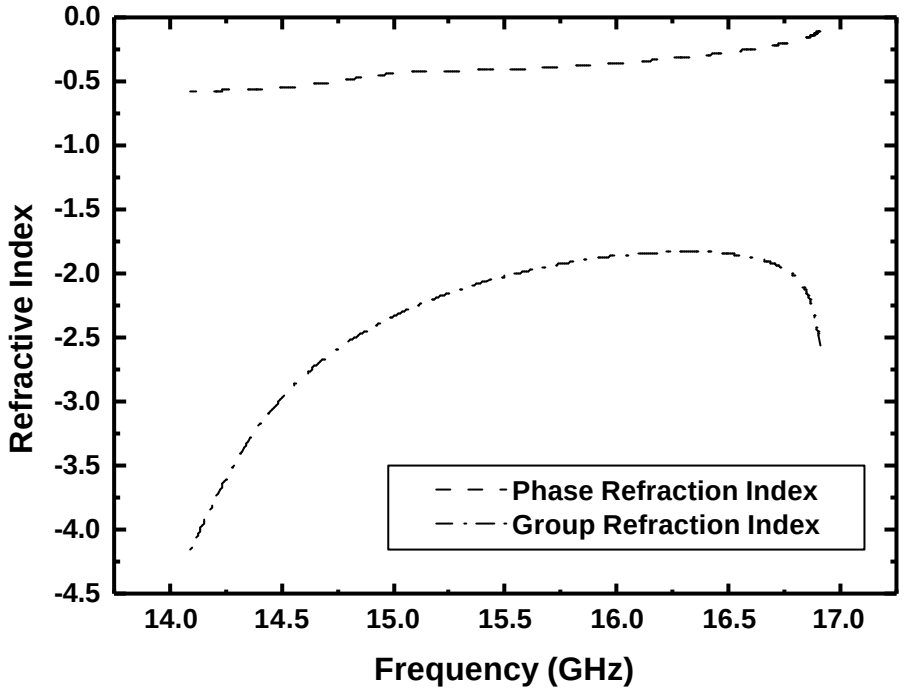

Fig. 18 The phase refraction indices are defined with the refraction angle of FDTD simulation results. the group refraction indices are derived from the photonic band structure.

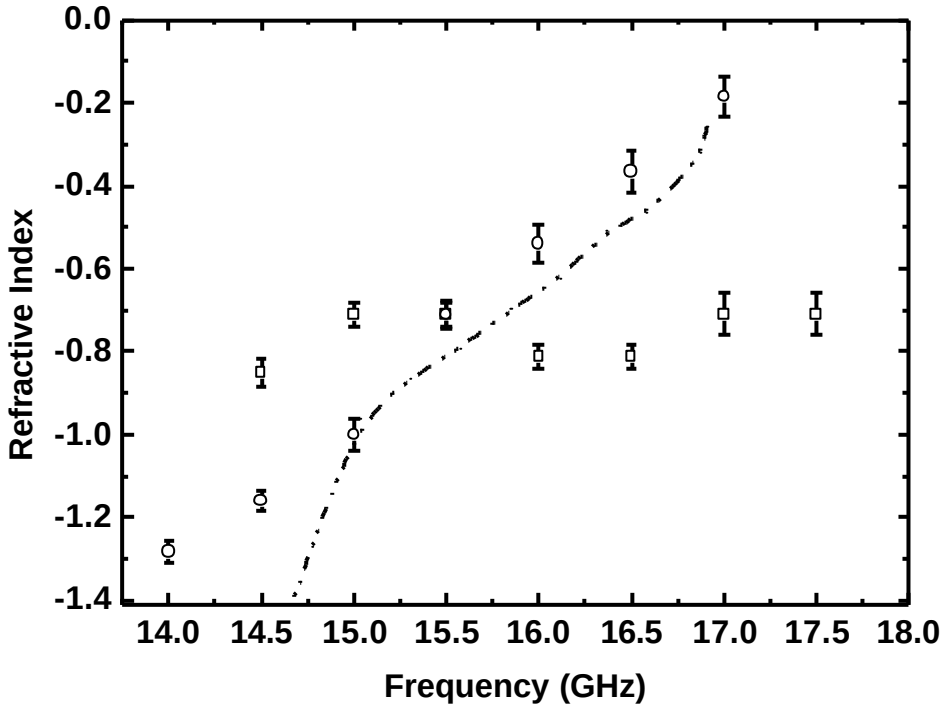

Fig. 19 Comparison between the experimental refractive indices and the theoretical effective refracive indices. The refractive indices of dash-dotted curve are defined with the product of the FDTD simulation results with the Snell's law and the group indices.

We have observed the negative refraction phenomenon with the FDTD algorism. The phase fronts can be refracted as the EM wave through the photonic crystal prism. We can define the phase refraction index with the Snell's law. From the photonic crystal band gap, we can get the group velocity with various wavelengths. Whereas, we show that only the product of phase index and group index has the physical meaning. The calculated product of phase index and group index derived from the FDTD algorism fit reasonably well with the experimental data. And, according to the extended $\mathbf{k} \cdot \mathbf{p}$ theory, the group velocity of EM waves in PC can be defined as the ratio of momentum to relativistic effect mass of a quasi-particle. The EM wave propagating in PC behaves like a massive quasi-particle. The phase refraction index is the same to the refraction factor with it. The simulation with the FDTD method told me this fact.

4-5 The negative refraction phenomenon

The fact that we can realize an arbitrary refractive index state leads to many possibilities for the control of light propagation. The most interesting point is that this realizes negative refraction, as illustrated in Fig. 20(a) This negative refraction leads to many anomalous light propagation phenomena. We show some examples: an imaging effect [Fig. 20(b)] and an open cavity formation [Fig. 20(c)]. In the latter case, there exist many closed optical paths running across the four interfaces which form a kind of an open cavity despite the fact that there is no reflecting wall surrounding the cavity. In the former case, light is emitted from a point source to a negatively refractive photonic crystal. Within the conventional paraxial-ray treatment, the refracted wave converges at another point in the photonic crystal. This means that objects in the left-hand space produce real images in the right-hand space. This imaging is fundamentally different from conventional imaging by a lens. Figure 21 schematically illustrates two types of imaging. Imaging by a lens is described by Newton's formula, in which the focal length is an important parameter. Magnification depends on the relative distance of an object from the lens and focus point. Therefore it only produces a 2D image on the focal plane and does not produce a 3D image. On the contrary, a negatively refractive photonic crystal produces a 3D image (if it is a 3D negatively refractive photonic crystal! by the mirror-inversion transformation $(x, y, z) \rightarrow (x, y, -b\,z)$ where $b = \mathrm{abs}\left(\mathrm{n}_{eff} / \mathrm{n}_0\right)$, which is different from Newton's formula. In addition, the lens imaging has a definite principal axis, but the present imaging has translational

symmetry in the boundary plane. In this sense, this imaging is rather close to imaging by a mirror. The apparent difference between a photonic crystal and a mirror is that the former produces a real image but the latter only produces a virtual image. This unique property is suggesting possibilities of 3D photographing by use of negatively refractive photonic crystals.

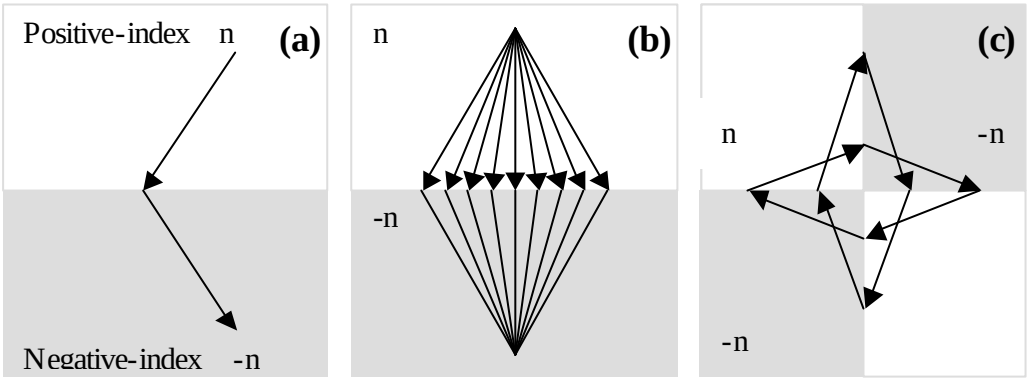

Fig. 20 Schematic diagrams of light propagation in negativelyrefractive photonic crystals: (a) negative refraction, (b) mirrorinverted imaging effect, and (c) formation of an open cavity.

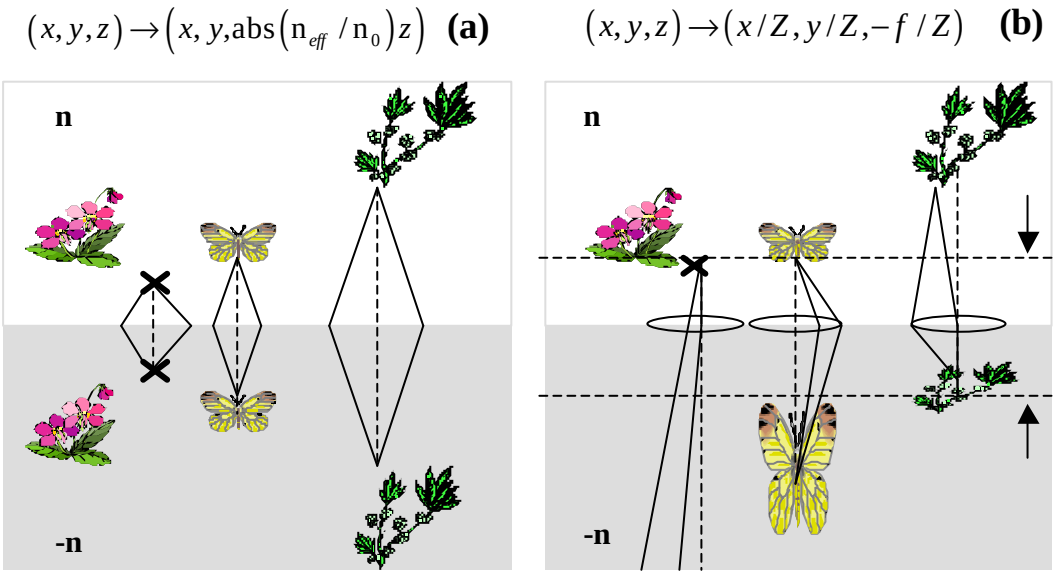

FIG. 21 Schematics of imaging by a negatively-refractive photonic crystal and imaging by a lens.

Chapter 5 Conclusion

We have observed the electromagnetic waves undergo negative refraction in a two-dimensional photonic crystal prism in microwave frequency regime. The negative refractive phenomenon displays in the negative state of photonic crystal band structure which can be solved with k.p theorem. The refraction phenomenon is derived form the refraction index, such as phase refraction index and group refraction index. By measuring the refraction angles of EM waves propagating through a PCP, and applying the Snell's law to the exit interface of PC and air, we deduced the negative refractive indices. The group index, calculated by taking gradient of the dispersion relation curve, disagrees with the experiment. And, The phase velocity is defined as the velocity of the propagation of an equi-phase surface. This velocity has a definite meaning, for example, for plane waves and spherical waves for which the equi-phase surface can be defined without ambiguity, in the photonic crystal, however, the equi-phase surface cannot be defined rigorously, since its eigenfunction is a superposition of plane waves. This means that the phase velocity cannot be defined appropriately in photonic crystal. Whereas, we show that only the product of phase index and group index has the physical meaning. The calculated product of phase index and group index derived from the extended $\mathbf{k} \cdot \mathbf{p}$ theory fit reasonably well with the experimental data. Thus, it is possible to reconstruct the photonic band structure from measurement of refraction angles for light propagation through the PC. And, according to the extended $\mathbf{k} \cdot \mathbf{p}$ theory, the group velocity of EM waves in PC can be defined as the ratio of momentum to relativistic effect mass of a quasi-particle. The EM wave propagating in PC behaves like a massive quasi-particle.

We have also observed the negative refraction phenomenon with the FDTD algorism. We show the refraction phenomenon is different from the conventional medium, such as glass. The phase fronts can be refracted as the EM wave through the photonic crystal prism. We can define the phase refraction index out of the photonic crystal prism with the Snell's law. From the photonic crystal band structure, we can get the group velocity with various wavelengths also. We show the product of phase index and group index was good match to our experimental result. And, according to the extended $\mathbf{k} \cdot \mathbf{p}$ theory, the group velocity of EM waves in PC can be

defined as the ratio of momentum to relativistic effect mass of a quasi-particle. The negative refraction phenomenon can be seen as the particle was trapped on the interference between the photonic crystal medium and the air. The thinking, the EM wave propagating in PC behaves like a massive quasi-particle, are an important confirmation that the speed of light is not violated by negative refraction.

"The EM wave propagating in PC behaves like a massive quasi-particle". "The phase refraction index and the group refraction index are the kinds of the refraction factors with it". We demonstrate this fact with FDTD method and k.p theorem.

References

[1] V. G. Veselago, ***Sov. Phys. Usp. 10, 509 (1968).***

[2] J. B. Pendry, ***Phys. Rev. Lett. 85, 3966 (2000).***

[3] J. B. Pendry, A. J. Holden, W. J. Stewart, and I. Youngs, ***Phys. Rev. Lett. 76, 4773 (1996).***

[4] D. R. Smith, W. J. Padilla, D. C. View, S. C. Nemat-Nasser, and S. Schultz, ***Phys. Rev. Lett. 84, 4184 (2000)***

[5] R. A. Shelby, D. R. Smith, and S. Schultz, ***Science 292, 77 (2001).***

[6] H. Kosaka, T. Kawashima, A. Tomita, M. Notomi, T. Tamamura, T. Sato, and S. Kawakami, ***Phys. Rev. B 58, 10096 (1998)***

[7] M. Notomi, ***Phys. Rev. B 62, 10 696 (2000).***

[8] S. Foteinopoulou, E. N. Economou and C. M. Soukoulis, ***Phys. Rev. Lett. 90, 107402 (2003).***

[9] C. G. Parazzoli, R. B. Greegor, K. Li, B. E. C. Koltenbah, and M. Tanielian, ***Phys. Rev. Lett. 90, 107401 (2003).***

[10] E. Yablonovitch, ***Phys. Rev. Lett. 58, 2059 (1987).***

[11] S. Kawakami, Electron. Lett. **33**, 1260 (1997).

[12] M. Notomi, T. Tamamura, Y. Ohtera, O. Hanaizumi, and S.Kawakami, ***Phys. Rev. B 61, 7165 (2000).***

[13] P. Halevi, A. A. Krokhin, and J. Arriaga, ***Phys. Rev. Lett. 82, 719(1999).***

[14] N. A. Nicorovici, R. C. McPhedran, and L. C. Botten, ***Phys. Rev. Lett. 75, 1507 (1993).***

[15] R. C. McPhedran, N. A. Nicorovici, and L. C. Botten, ***J. Electron.Waves Appl. 11, 981 (1997).***

[16] S.-Y. Lin, V. M. Hietala, L. Wang, and E. D. Jones, ***Opt. Lett. 21, 1771 (1996).***

[17] A. Yariv and P. Yeh, ***Optical Waves in Crystals*** ~Wiley, New York, **(1984)**

[18] J. P. Dowling and C. M. Bowden, ***J. Mod. Opt. 41, 345 (1994).***

[19] P. Yeh: ***J.Opt. Soc. Am. 69, 742 (1979)***

[20] K. Yee, ``Numerical solutions of initial boundary value problems involving Maxwell's equations in isotropic media," ***IEEE Transactions on Antennas and Propagation***, vol. AP-14, pp. 302-307, (1966).

[21] J. Adhidjaja and G. Horhmann, ``A Finite-Difference Algorithm for the Transient Electromagnetic Response of a Three-Dimensional Body," **Geophysics J. Int.,** ***vol. 98, pp. 233-242, 1989.***

[22] M. Piket-May and A. Taflove, ``Electrodynamics of Visible-Light Interactions with the Vertebrate Retinal Rod," **Optics Letters, *vol. 18, no. 8, pp. 568-570, 1993.***

[23] M. Celuch-Marcysiak and W. Gwarek, ``Higher order modeling of media interfaces for enhanced fdtd analysis of microwave circuits," in *24th European Microwave Conference*, vol. 24, (Cannes, France), pp. 1530-1535, September 1994.

[24] D. Sullivan, D. Borup, and O. Gandhi, ``Use of the Finite-Difference Time-Domain Method in Calculating EM Absorption in Human Tissues," *IEEE Trans. Biomed. Eng.*, vol. 34, no. 2, pp. 148-157, 1987.

[25] S. Caorsi, A. Massa, and M. Pastorino, ``Computation of Electromagnetic Scattering by Nonlinear Bounded Dielectric Objects: A FDTD Approach," *Microwave Opt. Technol. Let*, vol. 7, no. 17, pp. 788-790, 1994.

[26] K. Shlager and J. Schneider, ``A selective survey of the finite-difference time-domain literature," *IEEE Antennas and Propagation Magazine*, vol. 37, pp. 39-56, 1995.

[27]J. P. Berenger, A perfectly ma tcdhed layer for the absorption of electromagnetic waves, ***J. Comput. Phys., vol. 114, 1994, pp***

[28] N. F. Johnson and P. M. Hui, Phys. Rev. B 48, 10118 (1993); N. F. Johnson, P. M. Hui and K. H. Luk***, Solid State Commun. 90, 229 (1994).***

[29] K. M. Ho, C. T. Chan, and C. M. Soukoulis, ***Phys. Rev. Lett. 65, 3152 (1990).***

[30] S. C Cheng and W. F. Hsieh, Optics in information system, SPIE' s International technical group Newsletters, Aug. (2002); S. C Cheng and W. F. Hsieh, 73, Technical Digest of Optics in computing 2002.